UNIVERSITY OF TARTU
Faculty of Science and Technology
Institute of Bioengineering

Vjacheslav Morozov

A Comparative Life Cycle Assessment of Hydrogel and Polydimethylsiloxane (PDMS) Actuators

Master's Thesis (30 ECTS)

Curriculum Bioengineering

Supervisor(s):
Janno Torop, PhD
Alan Henry Tkaczyk, PhD
Cansu Özcan Kilcan, MSc

Tartu 2026

A Comparative Life Cycle Assessment of Hydrogel and Polydimethylsiloxane (PDMS) Actuators

Abstract: This thesis compares the environmental performance of a cellulose-based hydrogel actuator and a polydimethylsiloxane (PDMS) actuator. A cradle-to-gate life cycle assessment (LCA) was conducted for the production of a single 10 g actuator. Both systems were modeled in OpenLCA 2.4.1 using the Ecoinvent database version 3.11 and assessed with the Environmental Footprint (EF) v3.1 midpoint LCIA method. The results showed greater impacts from the PDMS actuator across most impact categories; for example, PDMS had about 166% higher climate change impact and about 118% higher non-renewable energy demand than the hydrogel actuator, while hydrogel generally showed a lower environmental profile.

Keywords: Life cycle assessment, soft robotics, hydrogel actuator, PDMS actuator, cellulose, environmental impact

CERCS: T150 Material technology; T270 Environmental technology, pollution control

Institute name: Institute of Bioengineering

Hüdrogeel- ja polüdimetüülsiloksaanist (PDMS) aktuaatorite võrdlev olelusringi hindamine

Lühikokkuvõte: Käesolevas lõputöös võrreldakse tselluloosipõhise hüdrogeelaktuaatori ja polüdimetüülsiloksaanist (PDMS) aktuaatori keskkonnamõju. Ühe 10 g aktuaatori tootmise hindamiseks viidi läbi hällist väravani olelusringi hindamine (LCA). Mõlemad süsteemid modelleeriti tarkvaras OpenLCA 2.4.1, kasutades Ecoinventi andmebaasi 3.11, ning neid hinnati Environmental Footprint (EF) v3.1 keskpunkti LCIA meetodiga. Tulemused näitasid, et PDMS-aktuaatoril oli suurem mõju enamikus mõjukategooriates; näiteks oli PDMS-i kliimamuutuse mõju ligikaudu 166% suurem ja taastumatute energiaressursside nõudlus 118% suurem kui hüdrogeelaktuaatoril, samas kui hüdrogeel näitas madalamat keskkonnaprofiili.

Võtmesõnad: Olelusringi hindamine, pehme robootika, hüdrogeelaktuaator, PDMS-aktuaator, tselluloos, keskkonnamõju

CERCS: T150 Materjalitehnoloogia; T270 Keskkonnatehnoloogia, reostuskontroll

TABLE OF CONTENTS

TERMS, ABBREVIATIONS AND NOTATIONS

BOD_5	Biochemical Oxygen Demand over 5 days
CAD	Computer-Aided Design
COD	Chemical Oxygen Demand
CTUe	Comparative Toxic Unit for ecosystems
CTUh	Comparative Toxic Unit for humans
DOC	Dissolved Organic Carbon
Ecoinvent	Life cycle inventory database used as the background database
EF v3.1	Environmental Footprint version 3.1 method
[EMIM][OAc] EmimOAc	1-ethyl-3-methylimidazolium acetate, also referred to as EMIMAc or
IL	Ionic Liquid
ISO	International Organization for Standardization
JRC	Joint Research Center
kBq U-235-Eq	Kilobecquerel Uranium-235 equivalent
kg CFC-11-Eq	Kilogram CFC-11 equivalent
kg CO_2-Eq	Kilogram Carbon dioxide equivalent
kg N-Eq	Kilogram Nitrogen equivalent
kg P-Eq	Kilogram Phosphorus equivalent
kg Sb-Eq	Kilogram Antimony equivalent
LCA	Life Cycle Assessment
LCC	Life Cycle Costing
LCI	Life Cycle Inventory
LCIA	Life Cycle Impact Assessment

MJ NCV	Megajoule, net calorific value
mol H^+-Eq	Mole Hydrogen ion equivalent
mol N-Eq	Mole Nitrogen equivalent
NMVOC	Non-Methane Volatile Organic Compounds
OpenLCA	Software environment used for LCA modeling
PDMS	Polydimethylsiloxane
S-LCA	Social Life Cycle Assessment
TOC	Total Organic Carbon
VOC	Volatile Organic Compound
wt%	Weight percent

INTRODUCTION

Modern robotics is no longer evaluated only by technical performance. As robots are used more commonly in research, medicine, and everyday technologies, their environmental impacts become increasingly important. Researchers now need to consider which materials robots use, how manufacturers produce them, how long the systems remain functional, and what happens to them after use. This change has led to growing interest in sustainable robotics, which focuses on detailed material management. Recent literature highlights using renewable and recycled raw materials as a necessary element for reducing the environmental burden of robotic systems (Miao & Bai, 2024).

The soft robotics field makes these questions especially important because material choice directly affects device function. Unlike conventional rigid robots, which usually rely on hard parts, soft robots use compliant materials to create movement and interaction. The replacement of the material with other alternatives can therefore influence not only sustainability but also flexibility. Soft robotic systems often draw inspiration from biological structures, where motion arises from the deformation of soft tissues rather than rigid mechanical assemblies. This makes soft robotics a useful platform for exploring bio-based, biodegradable, recyclable, or otherwise more sustainable materials. Despite this potential, many soft robotic systems still rely on conventional synthetic elastomers.

Actuators are the parts of a soft robotic system that turn an input signal or energy source into movement, deformation, or force. They are especially important in soft robotics because they determine how a device bends, expands, grips, or interacts with its surroundings. Silicone-based materials, including polydimethylsiloxane (PDMS), are still widely used for these components. They are relatively easy to process and show great working potential in many soft actuator designs. Recent soft robotics literature describes silicone as one of the most classical non-biodegradable materials in the field and notes that fluidic elastomer actuators remain popular because they are low-cost and mechanically reliable (AboZaid et al., 2024). PDMS and related silicone elastomers offer useful properties, including flexibility, stability, and processability. However, good technical performance does not automatically mean good environmental performance. For this reason, PDMS-based actuators need to be assessed quantitatively rather than judged only by their practical advantages.

Hydrogels have attracted attention as one possible alternative material family for soft robotics, especially for the actuators. These water-rich polymer networks combine many useful

properties, like softness, biocompatibility, and ionic conductivity. Those properties make them useful for bioinspired soft systems that interact with delicate environments (Park et al., 2024). Within this broad family of materials, cellulose-based hydrogels are particularly relevant from the environmental sustainability perspective. Researchers often discuss cellulose-based hydrogels as green soft materials with applications in soft robotics (Kundu et al., 2022). Recent studies also show that cellulose-containing hydrogels can support advanced soft-robotic functions (Nasseri et al., 2023). However, the renewable origin of cellulose does not automatically make a cellulose-based hydrogel actuator environmentally preferable. To become a functional hydrogel, cellulose often needs a combination with other functional materials. Since cellulose is difficult to dissolve in water and many conventional solvents, its processing often requires more active solvent systems like ionic liquids, N-methylmorpholine-N-oxide-based systems, or alkaline solvent routes (Protz et al., 2021).

Ionic liquids are often described as promising solvents because they are low-volatility and can, in principle, be reused. Still, their environmental performance depends on how they are produced. This creates the main problem addressed in this thesis. A material may appear sustainable because it is bio-based or derived from renewable feedstocks, but these characteristics do not fully describe the system's environmental burden. The main impacts may occur elsewhere, for example, during precursor production, solvent use, electricity demand, purification, or waste treatment. The same caution applies to PDMS-based systems. PDMS actuators offer significant technical advantages, but conventional silicone elastomers are typically not considered biodegradable or bio-based. Therefore, material substitution in soft robotics needs a quantitative environmental assessment rather than assumptions based only on material origin. Life cycle assessment (LCA) provides a suitable framework for the aforementioned comparison. It allows often overlooked environmental impacts to be examined within a defined system boundary and can include all the necessary impact types (European Commission, Life Cycle Assessment & the EF methods Comprehensive coverage of impacts. Used 13.03.2026). In the context of emerging soft robotic actuators, LCA helps move the discussion beyond broad labels such as “bio-based” or “synthetic” and instead shows where environmental burdens actually arise.

This thesis focuses on evaluating the environmental performance of two soft robotic actuator material routes using LCA: 1) a cellulose-based hydrogel actuator and 2) a PDMS-based actuator. The main research question of this thesis is whether the cellulose-based hydrogel

actuator can offer an environmentally preferable alternative to the conventional PDMS-based actuator when the full production system is considered with a life cycle approach.

The environmental assessment follows a cradle-to-gate perspective. It covers the raw material extraction, precursor production, material preparation, processing, and actuator manufacture up to the point where the finished component leaves the production stage. This boundary was selected because the main differences between the two actuator systems are expected to occur during material production and fabrication. The functionality of the two materials and their use phase are assumed to be the same. Therefore, beyond the manufacturing stage was not considered in this study.

1 LITERATURE REVIEW

1.1 LIFE CYCLE ASSESSMENT (LCA)

LCA is a standardized method used to evaluate the potential environmental impacts associated with a product, process, or system over its life cycle (Sala et al., 2016). In practical terms, the assessment is not performed individually at one stage, such as manufacturing or disposal, but follows an entire life cycle from raw material extraction through production and use to the end of life. Because it accounts for inputs and outputs at different stages, LCA helps identify where the main environmental burdens occur and makes it possible to compare alternatives on a broader basis than a single indicator such as energy use or carbon emissions alone (Sala et al., 2016). LCA helps reveal possible trade-offs and burden shifting across the life cycle. LCA is described as the core method for the environmental dimension of life cycle thinking and can be complemented by life cycle costing (LCC) and social life cycle assessment (SLCA) when economic and social aspects are also considered (Sala et al., 2016).

According to ISO 14040:2006 and ISO 14044:2006, LCA consists of four main phases (Table 1): goal and scope definition, life cycle inventory analysis, life cycle impact assessment, and interpretation (International Organization for Standardization, 2006a, 2006b). In the first phase, the purpose of the study is defined together with key methodological choices such as the functional unit, system boundaries, LCIA methods and the corresponding impact categories, assumptions, and data quality requirements (Sala et al., 2016). The inventory phase then focuses on collecting and quantifying all inputs and outputs in the defined system, including materials, energy, emissions, products, and waste flows. The impact assessment phase links these inventory flows to environmental impact categories and expresses them in common indicator units. In contrast, the interpretation phase evaluates the results in relation to the original goal and scope of the study and includes checks for completeness, consistency, sensitivity, and uncertainty.

Table 1. Main phases of LCA according to ISO 14040:2006 and ISO 14044:2006, with phase descriptions (International Organization for Standardization, 2006b, 2006a).

Phase	Main purpose
Goal and scope definition	Defines the purpose of the study, functional unit, assumptions, system boundaries, impact categories, and data quality requirements
Life cycle inventory analysis	Compiles and quantifies material and energy inputs, products, emissions, and waste flows
Life cycle impact assessment	Links inventory flows to impact categories and expresses them in comparable indicator units
Interpretation	Evaluates the results in relation to the goal and scope, including consistency, completeness, sensitivity, and uncertainty checks

Several methodological choices have strong influence on LCA results. Sala et al. identify five key aspects: the functional unit, the system boundary, multifunctionality, the choice of LCIA method, and the type and quality of data. It also points out that the modeling approach matters. Attributional LCA describes the physical flows associated with a product system as it exists. In contrast, consequential LCA is intended to describe how these flows may change in response to a decision or a change in demand. In that sense, attributional modeling is mainly accounting-oriented, while consequential modeling is more closely linked to comparative and future-oriented questions.

LCIA is the part of LCA in which inventory data are translated into environmental impact indicators. In other words, the material and energy consumptions, emissions, waste generation flows recorded during the inventory phase are linked to impact categories and expressed in common units, enabling the results to be interpreted in a broader context (Sala et al., 2016). This is what allows raw inventory data to be read not simply as emissions or resource use, but as potential contributions to climate change, eutrophication, acidification, toxicity, and other environmental problems. An important point in LCIA is that the results depend not only on the inventory itself but also on the chosen impact assessment method. Different methods are based on different modeling assumptions and may emphasize different categories or levels of aggregation. For this reason, the choice of the LCIA method is a methodological decision in its own, not just a technical step in the software.

1.2 ACTUATORS IN SOFT ROBOTICS

In soft robotics, the actuator is the element that produces motion or force by converting an external input into mechanical deformation. In contrast to conventional rigid robots, which typically generate motion through joints, hinges, and discrete mechanical assemblies, a soft actuator is often part of the system's body. This means that the actuator is not only responsible for motion but also directly shapes how the robot bends, contacts objects, distributes stress, and adapts to its surroundings. In this sense, the actuator is central to both the function and the material design of a soft robotic system (M. Li et al., 2022).

From a life cycle perspective, the link between material choice and actuator function matters. A soft actuator is not just a material sample. It is a working component made through a specific fabrication route. Its environmental profile can therefore depend on the material used, the processing steps, and the performance expected from the final actuator.

In the soft robotics literature, actuators are commonly discussed based on the working principle. One recent review of soft grippers groups grasping technologies into three broad categories: actuation, controlled stiffness, and controlled adhesion, and describes actuation as the direct mechanism by which the soft body produces motion and interacts with the target object. Fluidic elastomer actuators, for example, are described as one of the most established actuation classes and remain widely used because of their intrinsic compliance, straightforward fabrication, robustness, and the availability of low-cost elastomer materials. (Y. Zhang et al., 2025)

At a broader level, recent reviews of soft actuators emphasize that performance in this field is always tied to both materials and structures. Soft actuators have been developed for applications ranging from grippers and artificial muscles to wearables and medical devices. Still, their effectiveness depends on how material properties are coupled to geometry, internal architecture, and the selected activation mechanism (M. Li et al., 2022). This is why the literature does not treat actuation as a purely mechanical problem. Instead, it is usually framed as a combined question of material response, structural design, and fabrication strategy.

1.2.1 Cellulosic hydrogel actuator

Cellulose-based hydrogel actuators are a subset of stimuli-responsive hydrogel actuators. These soft material systems convert environmental or external stimuli into mechanical deformation. A hydrogel consists of a three-dimensional polymer network that can hold a large

amount of water while still behaving like a solid (Park et al., 2024). This combination of softness, elasticity, and hydration makes hydrogels especially attractive for soft robotics, where movement often comes from distributed deformation rather than from rigid joints, gears, or motors (H. Wang et al., 2025). Hydrogels are described as promising materials for bioinspired soft robots because they can respond to temperature, pH, humidity, ionic strength, and electric or magnetic fields(Park et al., 2024). A hydrogel actuator primarily operates by the movement of water, ions, or solvent within the polymer network. When a stimulus changes the interaction between the polymer chains and the liquid phase, the hydrogel can swell, bend, fold, or change shape (R. Wang et al., 2024). Uniform swelling usually causes expansion or contraction. Non-uniform swelling, in contrast, can produce directional bending or more complex shape transformation (Dong et al., 2024). For this reason, researchers often design hydrogel actuators as bilayers, gradient structures, patterned materials, anisotropic networks, or composites with regions that respond differently to the same stimulus (Dong et al., 2024). (Park et al., 2024) identify solvent uptake and release as one of the central mechanisms of hydrogel actuation, while other reviews show that the internal structure of the hydrogel can be just as important as its chemical composition (Ahmed, 2015). In simple terms, a hydrogel does not become an actuator just because it contains water, it becomes an actuator when researchers engineer ion transport to produce useful motion.

Figure 1 shows representative photographs of the cellulose-based hydrogel actuator material considered in this thesis. The images are included to illustrate the film-like morphology and flexibility of the hydrogel-based actuator route. They are not used as direct quantitative LCA inputs; the quantitative model is instead defined later through the foreground inventory and OpenLCA process system.

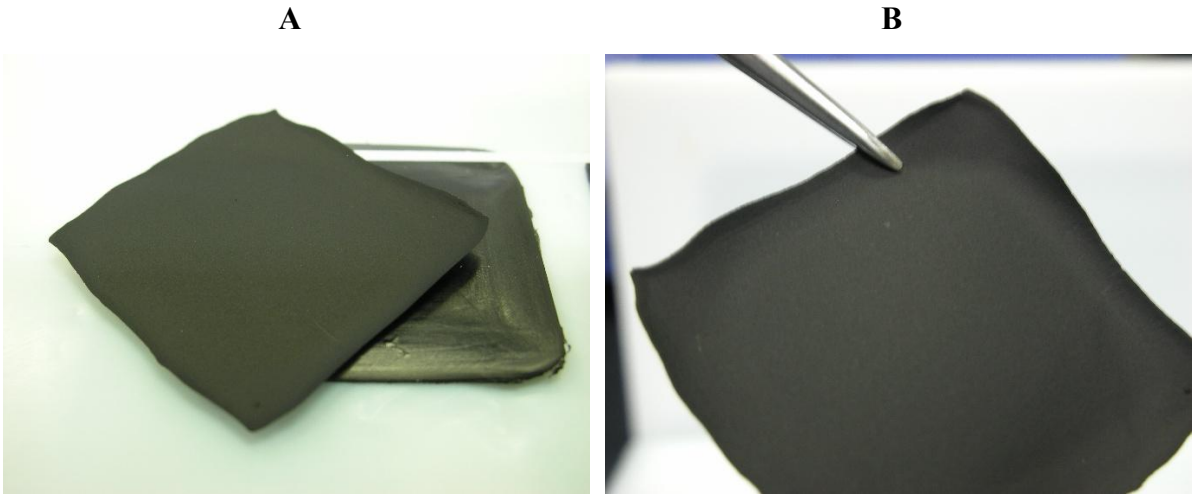

Figure 1. Representative cellulose-based hydrogel actuator material. (A) Cast hydrogel composite sheets and (B) flexible hydrogel film handled with tweezers. The images illustrate the soft, film-like morphology of the hydrogel actuator material considered in this thesis. Photographs taken by the author in collaboration with supervisor Janno Torop.

Considering cellulose, it is an important material in this field because of its biodegradability and biocompatibility when compared with other polymers. Which often presented as a green alternative for soft robotics (X. Li et al., 2025; López-Díaz et al., 2024; Trombino et al., 2023). However, raw cellulose fiber cannot usually act as a hydrogel actuator on its own. Native cellulose has strong intra- and intermolecular hydrogen bonding, which makes it difficult to dissolve in water and in many conventional solvents (Taokaew, 2023). To turn cellulose into a useful hydrogel actuator, it usually needs to be modified or combined with other materials. These steps help form a network that can absorb water, transport ions, and deform predictably (Szabó et al., 2023).

Next material which plays crutial role is ionic liquid (IL). It simply can dissolve or process cellulose more effectively than many conventional solvent systems. Imidazolium-based ionic liquids, including 1-ethyl-3-methylimidazolium acetate [C8H14N2O2], often written as [EMIM][OAc] are especially relevant because they can disrupt the hydrogen-bonding structure of cellulose and produce processable cellulose solutions or gels (Hassan & Mutelet, 2017). Some studies warn against treating ionic liquids as automatically sustainable only because they have low vapor pressure (Szabó et al., 2023). Their environmental relevance depends on how researchers produce, recover, recycle, and handle them, as well as on energy demand, toxicity, and solvent losses (Freire Ordóñez, Pontillo, et al., 2025; Kraemer et al., 2023). This distinction

matters because many bio-based hydrogel systems still depend on advanced solvents and multi-step processing.

A preparation logic for cellulose ionogel actuator is shown in Figure 2. This type of route is relevant to this thesis because it links the same material families that later appear in the LCA model: cellulose, an imidazolium-based IL, activated carbon, a water-based phase-inversion process, and a layered actuator structure. The figure is used as a conceptual example from the literature rather than as a direct inventory dataset.

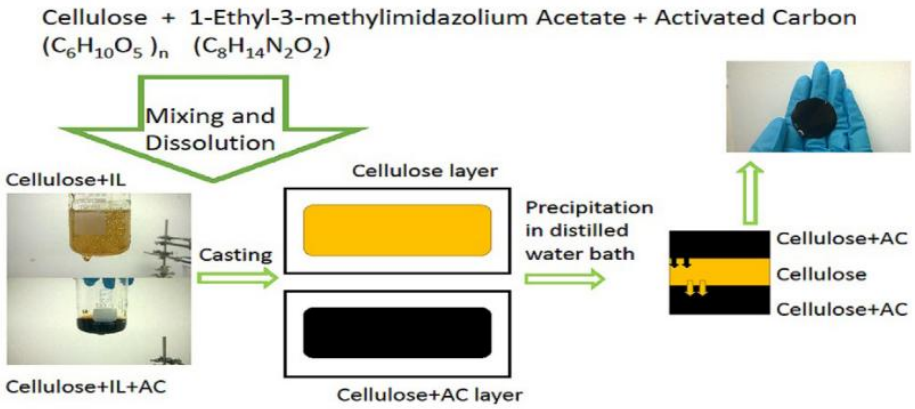

Figure 2. Schematic illustration of the preparation of regenerated cellulose-ionogel low-voltage actuators via phase inversion method. Reprinted from Colloids and Surfaces B: Biointerfaces, Vol. 161, Nevstrueva et al., "Natural cellulose ionogels for soft artificial muscles," pp. 244–251, Copyright © 2017 Elsevier B.V., with permission from Elsevier under License No. 6271871509316.

Cellulose-based hydrogel actuators can respond to various stimuli. Some systems respond to temperature, pH, light, ionic conditions, or electric fields. Electroactive cellulose-based hydrogels are especially relevant for soft robotics because electrical stimulation is relatively easy to control and can be integrated with sensors, electrodes, and electronic circuits. In ionic electroactive systems, deformation often comes from ion migration or electroosmotic flow. Qian et al., 2023 showed that ion doping can enhance the electroactive response of cellulose nanofibril actuators, as ion migration plays a central role in their bending mechanism. More recent work on nanocellulose-based ionic soft actuators also uses cellulose nanofibres, ionic liquids, and ion-exchange membranes to improve conductivity and actuation performance (X. Li et al., 2025; Qian et al., 2023). Nasseri et al., 2023 provided a useful example of how cellulose can contribute to programmable hydrogel actuation. They developed nanocomposites based on cellulose nanocrystals and zwitterionic hydrogels for small-scale soft robotics. Their work shows that cellulose can do more than reinforce a hydrogel.

The main appeal of cellulosic hydrogel actuators comes from their combination of several useful features: renewable polymer origin, high water content, biocompatibility, tunable swelling, ionic conductivity, and the possibility of programmed deformation. However, the literature also points to clear limitations. Hydrogels can dry out, lose water, change their mechanical properties over time, respond slowly when diffusion distances are large, or show low mechanical strength. Cellulose-based systems can reduce dependence on synthetic

petrochemical polymers, but they may still require energy-intensive processing. Recent LCA work on [EMIM][OAc]-processed lignocellulosic films shows that electricity use, ionic-liquid production, and solvent recovery can strongly influence the environmental burden of ionic-liquid routes (Freire Ordóñez, Pontillo, et al., 2025). For this reason, cellulose-based hydrogel actuators should be seen as promising bio-based soft actuator systems, but not automatically as low-impact environmentally-friendly product. Their environmental profile still depends on the processing route, additives, water use, solvent management, and electrode materials.

1.2.2 Polydimethylsiloxane (PDMS) actuator

PDMS has become one of the standard elastomers in soft robotics and related fields, including microfluidics, flexible electronics, wearable devices, biomedical systems, and electroactive polymer actuators. Its wide use is not accidental it combines several properties that are difficult to find together in one material: it is flexible, chemically stable, thermally stable, optically transparent, and biocompatible in many applications. It is also relatively easy to process, especially by casting or molding, which makes it attractive for laboratory-scale soft devices and prototype development. (Miranda et al., 2022)

Most commercial PDMS systems are supplied as two-part materials, usually a base polymer and a curing agent (Y. Zhang, Adam, et al., 2024). After mixing and curing, these components form a crosslinked silicone elastomer. The final properties of this elastomer are not fixed. They depend on the aspects like mixing ratio, curing temperature and post-processing conditions (Sales et al., 2021). As a result, you can adjust properties like stiffness, elongation or many other for different soft-device applications. So this tunability explains why PDMS appears in so many forms.

The term "PDMS actuator" covers a broad range of devices. In some systems, PDMS forms the body of a pneumatic actuator. In others, it acts as the dielectric layer in a dielectric elastomer actuator or the elastic host in a multifunctional hybrid system (S. Li et al., 2023). These actuators may respond to pressure, voltage, heat or even electric fields. What links them is the same material logic: PDMS provides a soft and deformable structure, while the selected stimulus creates motion through mechanical, electrical, thermal, or interfacial effects (El-Atab et al., 2020). This material logic is especially important in soft robotics. Conventional machines usually rely on joints, gears, and motors. Soft actuators follow a different approach. They use deformable materials to create movement directly in the body of the device, what allows actuator to interact more gently with fragile objects or biological tissues (Eyvazian et al., 2026).

With all those aspects PDMS stays as a benchmark material in this area. It is not the most sustainable material, and it is not always the highest-performing material, but it provides a stable and well-understood platform for many soft robotic designs.

A literature example is shown in Figure 3. The figure presents a flower like PDMS based soft actuator in two views: a side view showing the opened three-dimensional deformation and a top view showing the illuminated actuator structure. In this type of system, PDMS works as the compliant elastomeric matrix, while the functional graphene/PDMS layer enables light-responsive deformation. This example is not used as a direct input to the LCA inventory in this thesis. Instead, it is included to illustrate why PDMS remains a common platform in soft-robotic actuator design: it can be processed into thin films, combined with functional fillers, patterned into biomimetic geometries, and transformed into controlled, shape changing structures.

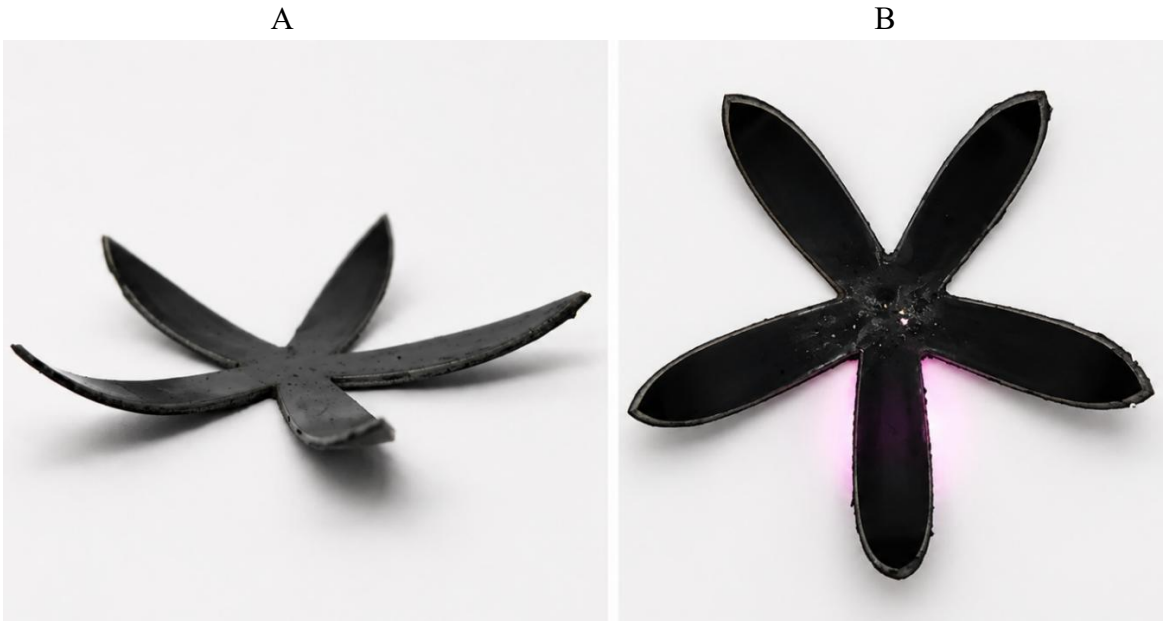

Figure 3. Literature example of a PDMS based biomimetic soft actuator. Two views of a flower-like graphene/PDMS bilayer actuator: (A) side view showing opened three-dimensional deformation and (B) top view showing the actuator during light induced activation. The figure illustrates the use of PDMS as a flexible elastomeric matrix in a shape-programmable soft actuator system. It is used as a qualitative literature example and is not part of the LCA inventory model. Reproduced in part with permission from Chen et al., (2023). Multifunctional actuator based on graphene/PDMS composite materials with shape programmable configuration and high photothermal conversion capability. ACS Applied Materials & Interfaces, 15(26), 31917-31926. Copyright 2023 American Chemical Society.

Dielectric elastomer actuators are one of the clearest examples of PDMS-based actuation. In this type of device, a soft dielectric elastomer sits between two compliant electrodes (Katzer et al., 2022). When voltage is applied, electrostatic Maxwell stress compresses the elastomer in thickness and causes lateral expansion. If the actuator has a suitable from this expansion can be converted into controlled motion. More recent reviews also treat dielectric elastomer, fluidic, and electrostatic actuators as important technologies for future soft robotic systems (Molla et al., 2026).

The mechanical behaviour of PDMS has a direct influence on actuator performance. PDMS can deform under large strain, but it does not behave like a perfectly linear elastic material. It can affect displacement, response time, energy efficiency, and long-term stability. Teixeira et al., 2021 show that PDMS properties vary considerably with formulation and processing conditions. This matters in soft robotics because even a small change in stiffness can alter stability. For this reason, a PDMS actuator is best understood as a material-structure system. The polymer formulation defines the elastic body, while geometry and functional layers determine how that body moves (Katzer et al., 2022). Electrodes create another major challenge in PDMS-based electroactive actuators. A soft elastomer can only deform freely if the electrode system deforms with it. A rigid electrode may crack, restrict motion, or suppress the intended deformation (Q. Zhang et al., 2025). A poorly bonded electrode may delaminate during repeated cycling. In dielectric elastomer actuators, the electrode must conduct electricity while remaining mechanically compliant. For this reason, the literature often discusses carbon, graphene, liquid metals, stretchable metal films, conductive polymers, and ionically conductive gels as possible electrode or functional-layer materials (S. Li et al., 2025). The electrode is therefore not just an electrical contact. It forms part of the actuator's mechanical design. Even when the PDMS body remains intact, the actuator can fail if the electrode loses conductivity, adhesion, or mechanical compatibility. Surface behaviour adds a further complication. PDMS is naturally hydrophobic, so liquids, coatings, adhesives, and conductive layers do not always spread or bond well on its surface (S. Li et al., 2023). This issue appears frequently in PDMS research because many devices require stable contact between PDMS and another material, such as an electrode, hydrogel, adhesive, coating, or biological interface(S. Li et al., 2023).

Despite these challenges, PDMS has clear practical advantages. It is easy to mould, has excellent resistance to biodegradation, biocompatibility, and forms flexible devices without complex machining, which makes its use in soft robotics possible (Miranda et al., 2022). Compared with many hydrogels, PDMS also keeps its shape more reliably in air because it

does not need high water content to remain soft. It can be stored and handled more easily in dry conditions, and it is less vulnerable to dehydration (Y. Zhang, Adam, et al., 2024). At the same time, PDMS has limitations that are difficult to ignore. Low dielectric constant compared with some high-performance elastomers, its hydrophobicity complicates coating and bonding, and its tendency to absorb small hydrophobic molecules can also create problems in chemical and biomedical applications (S. Li et al., 2023).

From an environmental sustainability perspective, PDMS should be distinguished from bio-based material routes because conventional PDMS is a synthetic silicone rubber belonging to organosilicon polymers, whereas natural additives such as beeswax are derived from biological sources. Although PDMS-based composites can be modified with biodegradable natural components, the PDMS matrix itself remains a synthetic silicone material (Ariati et al., 2024).

2 THE AIMS OF THE THESIS

1. To evaluate whether the cellulose-based hydrogel actuator can represent an environmentally preferable alternative to the conventional PDMS-based actuator within the defined cradle-to-gate system boundary.
2. To contribute to the application of life cycle assessment methodology to early-stage emerging soft robotic actuator materials.
3. To identify the main environmental hotspots within each production route.
4. To develop a cradle-to-gate life cycle inventory for a cellulose-based hydrogel actuator and a PDMS-based actuator.
5. To assess and compare the environmental impacts of both actuator systems using the EF v3.1 midpoint impact assessment method.

3 EXPERIMENTAL PART

3.1 MATERIALS AND METHODS

3.1.1 Goal and scope definition

This LCA study was designed to evaluate and compare the potential environmental impacts of the laboratory-scale production of two soft robotic actuator systems: a Cellulosic Hydrogel Actuator and a PDMS Actuator. The assessment was developed as part of the experimental methodology of this thesis in order to connect the material selection and fabrication route of the actuators with their environmental performance. A laboratory-scale assessment was selected because the cellulose-based hydrogel actuator represents an emerging material route that has not yet been commercialized. As a result, available data mainly describe material preparation and actuator fabrication at the experimental scale rather than full industrial production. This LCA was structured according to the standard four-step LCA framework (section 1.1): goal and scope definition, life cycle inventory, life cycle impact assessment, and interpretation.

3.1.1.1 Goal of the study

The main goal of this LCA is to quantify the environmental profile of the hydrogel and PDMS actuators' lab-scale production routes modeled in this work and to identify which materials and production steps contributed most strongly to the overall impacts.

The research gap addressed in this assessment is the limited availability of dedicated environmental and life cycle assessment data for cellulosic hydrogel actuators. Although cellulose-based hydrogels are often touted as promising, bio-based, and potentially more sustainable materials for soft robotics, their environmental performance cannot be evaluated solely based on their renewable origin. The production of a functional cellulosic hydrogel actuator may also involve ionic liquids, activated carbon, coating materials, electricity use, water-intensive processing, wastewater generation, and other auxiliary inputs. Therefore, an environmental assessment at the level of the complete actuator production route is needed.

The study was designed as a comparative, production-focused LCA between a cellulose-based hydrogel actuator and a PDMS-based actuator. The PDMS actuator was chosen as the conventional benchmark material. Both systems were modeled as actuator systems with the

same assumed function and comparable modeling logic, allowing the two production routes to be evaluated consistently.

The specific objectives of the assessment were:

- To translate the experimental fabrication routes of both actuators into structured OpenLCA product systems.
- To quantify the material, energy, water, transport, waste, wastewater, and emission flows associated with the production of one actuator.
- To compare the environmental performance of the hydrogel-based actuator and the PDMS-based actuator under the same functional unit.
- To identify environmental hotspots within each actuator production system.
- To support the discussion of whether the cellulosic hydrogel route can represent a more environmentally favorable alternative to the PDMS-based route within the defined system boundary.

3.1.1.2 Functional unit and Reference flow

The functional unit was defined as:

"**One 10 g soft robotic actuator intended to generate movement or deformation in a soft robotic body.**"

The 10 g mass was selected as the modeling unit for the experimental actuator systems used in this thesis. This functional unit was applied to both the Cellulosic Hydrogel Actuator and the PDMS Actuator to compare two production routes for the same basic actuator function.

The reference flows used to represent this functional unit in the two product systems are shown in Table 2.

Table 2. Reference flows used for the two actuator systems

System	Reference flow	Amount
Cellulosic Hydrogel Actuator	Ready hydrogel actuator	0.010 kg
PDMS Actuator	Ready PDMS actuator	0.010 kg

All material, energy, transport, water, and waste inputs were scaled to the production of one 10 g actuator. Therefore, the final results of the LCA models represent the environmental impacts associated with the production of one actuator, rather than one kilogram of material or one isolated material component (section 3.2).

3.1.1.3 System boundary

The system boundary was defined as a cradle-to-gate (Figure 4 and 5). It includes upstream production of materials and energy carriers, transport of selected input materials, and the laboratory-scale fabrication processes required to obtain the final 10 g actuator. The model ends at the point where the actuator is produced, cleaned, stabilised, tested, and ready as the final laboratory-scale actuator.

The Cellulosic Hydrogel Actuator model was structured around the production of a cellulose-based hydrogel material and its transformation into a final actuator. The model includes the production of 1-ethylimidazole, the production of an imidazole-based acetate ionic liquid proxy corresponding to 1-ethyl-3-methylimidazolium acetate, heating of the ionic liquid, mixing with cellulose fiber, regeneration, precipitation, filtration, washing, purification, phase separation and gelification, shaping, electrode coating, and final quality control. The main material and process inputs include cellulose fiber, ionic liquid, activated carbon, deionized/process water, electricity, acrylic binder, deposited selective coating, transport, wastewater treatment, and inert waste treatment.

The diagram in Figure 4 shows the foreground production route used to build the hydrogel actuator model in OpenLCA. Input materials, such as ionic liquids, cellulose fibers, activated carbon, auxiliary components, water, electricity, and transport, are linked to the relevant production steps. The process chain proceeds from ionic liquid heating and cellulose mixing to hydrogel regeneration, precipitation, filtration, washing, purification, gelification, shaping, electrode coating, and final quality control. Secondary flows, such as wastewater and inert waste from shaping losses, are shown as outputs from the relevant stages. The final reference flow is one 10 g Cellulosic Hydrogel Actuator.

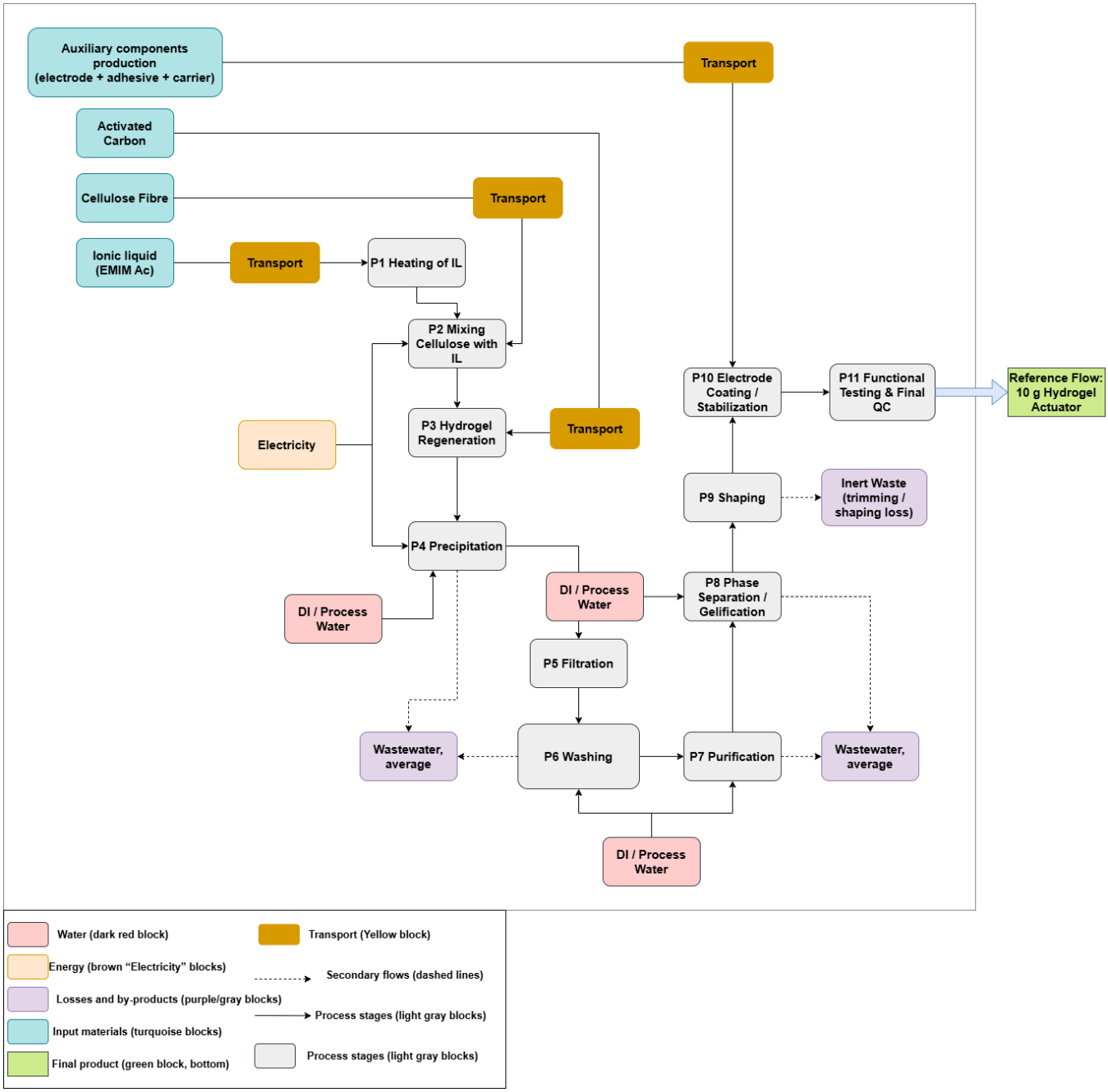

Figure 4. Process flow diagram of the Cellulosic Hydrogel Actuator system. The diagram was created manually by the author using draw.io based on the foreground OpenLCA model developed in this thesis. It shows the main process stages, material inputs, electricity and water inputs, transport flows, secondary flows, wastewater and waste outputs, and the final reference flow of one 10 g Cellulosic Hydrogel Actuator.

The PDMS Actuator model was structured around the production of a PDMS-based actuator body and its assembly with auxiliary electrode-related components. The foreground chain includes PDMS mixing with base and curing agent, casting and shaping by molding, thermal curing, replica removal and trimming, surface cleaning before coating, electrode application

and final shaping, cleaning, post-curing or stabilization, and functional testing. Auxiliary components, including the electrode, carrier, and adhesive materials, were modeled as a separate foreground process and connected to the assembly stage. The deposited selective coating was also modeled separately and linked to the auxiliary component route. The main material and process inputs include polydimethylsiloxane, an organic chemical proxy for the curing agent; methanol; deionized water; acrylic binder; deposited selective coating; electricity; transport; plastic waste treatment; wastewater treatment; and methanol emissions to water.

The diagram in Figure 5 shows the foreground production route used to build the PDMS actuator model in OpenLCA. The process starts with PDMS mixture preparation and proceeds through molding, thermal curing, trimming, surface cleaning, electrode application, final shaping, cleaning, post-curing, and functional testing. Auxiliary components and the deposited selective coating are included as separate upstream foreground inputs. The diagram also shows electricity use, deionized/process water, methanol use, transport, plastic waste, wastewater, and methanol emission to water. The final reference flow is one 10 g PDMS Actuator.

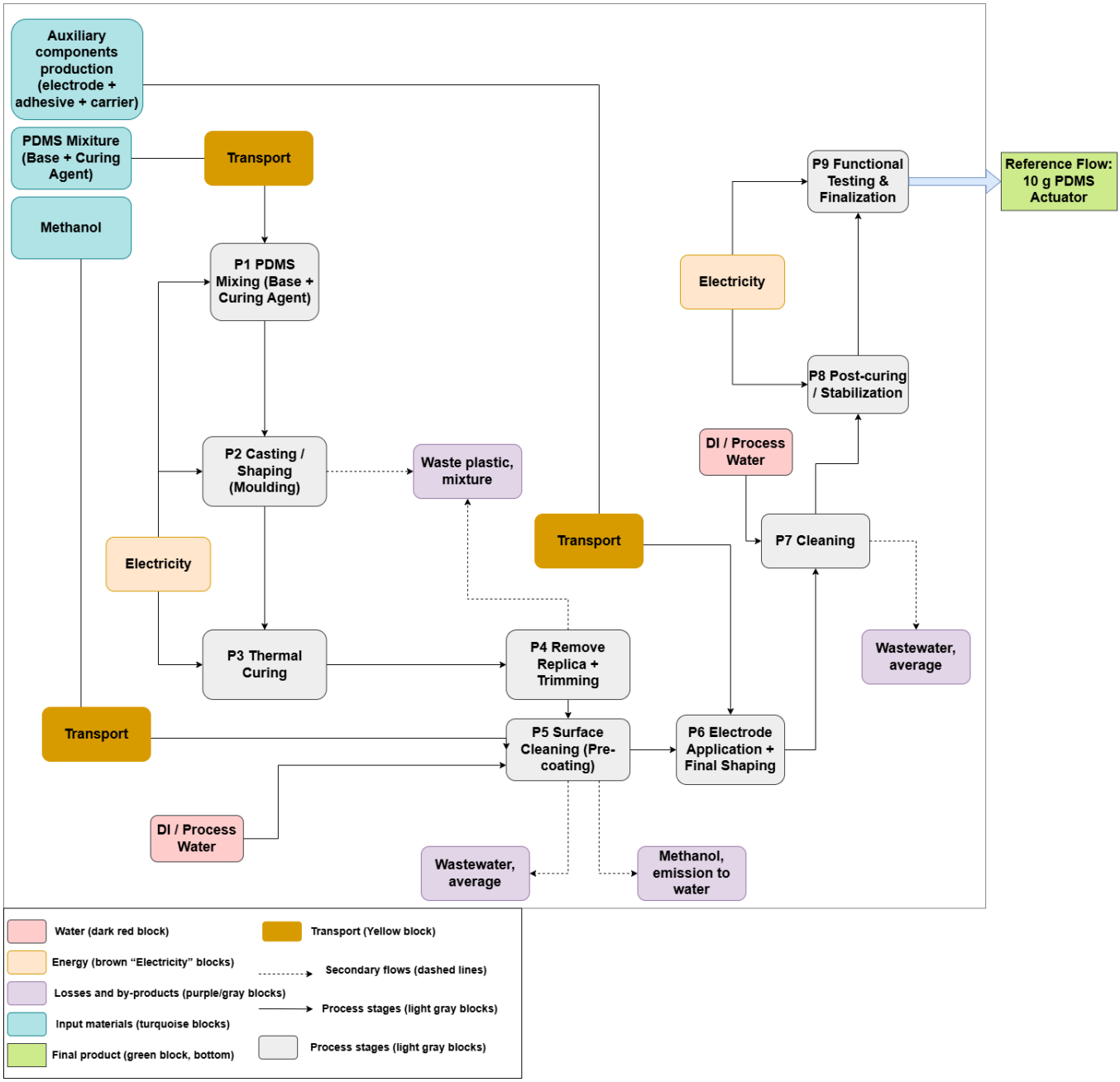

Figure 5. Process flow diagram of the PDMS Actuator system. The diagram was created manually by the author using draw.io based on the foreground OpenLCA model developed in this thesis. It shows the main process stages, material inputs, electricity and water inputs, transport flows, secondary flows, wastewater and waste outputs, methanol emission to water, and the final reference flow of one 10 g PDMS Actuator.

Transport was included as a foreground input for selected materials assumed to be delivered from Germany. A distance of 1600 km was applied and modeled using a freight lorry dataset corresponding to a 16-32 metric ton diesel EURO 6 lorry. In OpenLCA, transport was entered in kg·km, based on the mass of the transported material. This allowed the model to account for

the environmental impact of material delivery without attempting to reconstruct the complete global supply chain for every background material. The flow diagrams were used not only as illustrations, but also as a modeling guide for constructing the OpenLCA product systems. They define the sequence of foreground processes, the position of material and energy inputs, the formation of intermediate flows, and the location of waste and wastewater outputs. This was important because the two systems differ not only in material composition but also in production logic. The hydrogel system involves several water-intensive preparation and purification steps, while the PDMS system includes polymer mixing, curing, trimming, surface cleaning, and post-curing. The foreground inventory was therefore based on the experimentally defined fabrication routes, while the background inventory was supplied by Ecoinvent 3.11. Together, these foreground and background elements form the system boundary summarized in Table 3. Additional assumptions were applied where direct measurements or exact datasets were unavailable. These assumptions included the use of proxy datasets for specific materials, the use of selected waste and wastewater treatment datasets, and the inclusion of foreground transport for materials delivered from Germany. Material losses were included where they appeared in the OpenLCA model, such as trimming losses, shaping losses, plastic waste, wastewater, and methanol emission to water.

Table 3. Processes included in the system boundary

Included in the system boundary	Description
Raw material production	Background production of chemicals, polymers, cellulose fibre, ionic liquid precursors, PDMS-related inputs, coating materials, binders, water, and other auxiliary inputs
Transport	Transport of selected materials assumed to be delivered from Germany over a distance of 1600 km
Laboratory fabrication	Mixing, heating, casting, curing, regeneration, precipitation, washing, purification, gelification, shaping, coating, cleaning, stabilisation, and final testing steps
Energy inputs	Electricity and heat required for modelled production steps
Water inputs	Deionised water and process water used during precipitation, washing, purification, cleaning, and gelification-related steps
Waste and wastewater	Wastewater, plastic waste, inert waste, trimming losses, and methanol emission to water where included in the OpenLCA model
Final product	One 10 g Cellulosic Hydrogel Actuator or one 10 g PDMS Actuator

The processes excluded from the system boundary are summarized in Table 4. The use phase and end-of-life phase were not modeled as separate life cycle stages. This boundary choice was made because the study focuses on the production and material comparison of two actuator systems. Reliable data on long-term use, service lifetime, number of actuation cycles, repair rates, and disposal routes were not experimentally determined. Therefore, the end-of-life phase is considered a study limitation rather than a separate modeled scenario. Other exclusions were related to processes outside the physical production boundary or flows that were not consistently measured across both systems.

Table 4. Processes excluded from the system boundary

Excluded from the system boundary	**Reason for exclusion**
Use phase	No experimentally validated lifetime or actuation-cycle scenario was available
End-of-life	Disposal and recycling routes were uncertain for laboratory-scale prototypes
Laboratory infrastructure	Building operation, laboratory benches, ventilation, and general infrastructure were outside the scope
Capital equipment	Production of balances, ovens, moulds, computers, and laboratory tools was not included
Human labour	Manual work was not treated as an environmental flow
CAD modeling and software use	Digital design work was outside the physical production boundary
Packaging	Packaging was not consistently measured for all materials and was not central to the research question

3.1.1.4 OpenLCA model implementation

The LCA model was implemented in OpenLCA version 2.4.1 using Ecoinvent cut-off version 3.11 as the background database. The foreground systems were built manually from the experimental production routes developed in this thesis, while the background processes were linked to the Ecoinvent datasets through selected providers. These background datasets included material production, chemical production, polymer production, electricity, heat, transport, water supply, wastewater treatment, and waste treatment processes.

Each step in the life cycle was entered into OpenLCA as an individual foreground process with defined input and output flows. Intermediate product flows linked successive production stages, and the final output flow represented the completed actuator. This structure allowed for tracking how material costs, energy consumption, water consumption, transportation, and waste streams impacted the final environmental profile of each actuator system. Where available, background datasets were selected from the Ecoinvent Cut-off system model. The same modeling logic was applied to both actuator systems to maintain consistency between the

hydrogel-based and PDMS-based routes. When exact datasets for specific experimental materials were unavailable, proxy datasets were selected based on chemical, functional, or technological similarity. Literature sources and consultations with a specialist supervisor supported the selection of these proxies.

3.1.2 Life cycle inventory analysis

The life cycle inventory analysis quantified the material, energy, water, transport, waste, wastewater, and emission flows used in the two actuator product systems. The model structure, reference flows, system boundary, and OpenLCA implementation were defined in Section 3.1; therefore, this section focuses only on the inventory values used for the two systems and on the justification of the main modeling assumptions. All values reported in this section are scaled to the production of one 10 g actuator, corresponding to the reference flow defined in Section 3.1.1.2.

Supporting data for chemical production, material ratios, proxy selection, and equipment energy were taken from literature inventories, technical datasheets, equipment specifications, and specialist consultation. When exact datasets were unavailable, proxy datasets were selected and used based on chemical, functional, or technological similarity, a common approach in LCI modeling of emerging or laboratory-scale systems. (Tjokro, 2023) applied a similar approach in an LCA of a microfluidic device: unavailable Ecoinvent data were supplemented with literature, expert input, proxy datasets, and equipment-based electricity estimates.

3.1.2.1 Data sources and calculation rules

The inventory was divided into direct foreground data and supporting background or proxy data. Direct foreground data are the manually entered process values in the OpenLCA model for this thesis. These include the masses of the actuator materials, direct electricity inputs, water inputs, transport inputs, intermediate flows, waste flows, and final actuator outputs. Supporting data include upstream inventories for ionic liquid and 1-ethylimidazole production, the PDMS base-to-curing-agent ratio, interpretations of acrylic binder and coating inputs, and electricity allocation for oven-based curing and stabilization. Table 5 summarises the sources used to construct and justify the life cycle inventory.

Table 5. Main data sources used for Life Cycle Inventory modeling

Inventory data group	**Application in this study**	**Where reported**	**Role in the model**
Foreground actuator process data	Material, water, electricity, transport, waste, wastewater, and emission flows	Sections 3.1.2.3 and 3.1.2.5 (Tables S4 and S8); Sections 3.1.2.8 and 3.1.2.9 (Tables S10 and S11)	Primary inventory data normalized to one 10 g actuator
Ionic liquid production	Production of 1-ethyl-3-methylimidazolium acetate	Section 3.1.2.2 (Tables S1 and S2)	Supporting upstream chemical process
1- ethylimidazole production	Precursor production for ionic liquid synthesis	Section 3.1.2.2 (Table S3)	Supporting upstream precursor process
PDMS formulation	PDMS base and curing-agent mass ratio	Section 3.1.2.5 (Table S8)	Validation of the 10:1 PDMS ratio
PDMS curing and stabilization electricity	Oven electricity for thermal steps	Section 3.1.2.6 (Table 6)	Equipment-based electricity calculation

Detailed supporting inventories and scaled datasets are provided in the Supplementary Information [S1-S11].

The transport input for selected delivered materials was calculated as:

$$Transport\ input(kg * km) = material\ mass\ (kg) * 1600\ km$$

The conversion from water mass to wastewater volume was calculated using:

$$V = \frac{m}{\rho}$$

Where the density of water was assumed to be:

$$\rho_{water} = 1000\ kg/m^3$$

Thus, a water input of 0.010 kg corresponds to:

$$\frac{0.010\ kg}{1000\ kg/m^3} = 1.0 * 10^{-5}\ m^3$$

This conversion was used for the hydrogel precipitation, washing, purification, and phase separation/gelification steps.

3.1.2.2 Inventory for ionic liquid and precursor production

The hydrogel route uses an imidazole-based acetate ionic liquid proxy, 1-ethyl-3-methylimidazolium acetate. The production inventory for this ionic liquid was taken from supplementary LCI data for lignocellulosic film production with ionic liquids (Freire Ordóñez, Rozaria, et al., 2025 (Supplementary material)). Original inventory is reported per 1 kg of ionic liquid and includes dimethyl carbonate, acetic acid, 1-ethylimidazole, electricity, heat, carbon dioxide emissions, and wastewater. The complete 1 kg inventory is provided in Table S1.

In the hydrogel actuator model, the ionic liquid input was 0.00755 kg per actuator. Therefore, the upstream ionic liquid inventory was scaled by a factor of 0.00755. The scaled ionic liquid production inventory is provided in Table S2.

No ionic liquid recovery was modeled. The ionic liquid was therefore treated as consumed or lost during the laboratory-scale preparation. This is a conservative modeling assumption because an optimized future process with measured ionic liquid recovery could reduce the environmental burden associated with ionic liquid production.

The precursor, 1-ethylimidazole, was modeled using a separate literature review on the production of imidazole derivatives. The supporting inventory includes glyoxal, formaldehyde, ammonia, ethylamine, water, electricity, heat, wastewater, VOCs, and related output flows (Y. Zhang, Liu, et al., 2024). The full precursor inventory is provided in Table S3.

3.1.2.3 Inventory of the Cellulosic Hydrogel Actuator

The Cellulosic Hydrogel Actuator foreground inventory includes ionic liquid, cellulose fiber, activated carbon, deionized water, acrylic binder, selective coating, electricity, transport, wastewater, shaping loss, and the final actuator output. The detailed stepwise foreground inventory for all hydrogel processes is provided in Table S4.

The cellulose input was checked against data on cellulose/ionic-liquid dope. The supporting ionic-liquid LCI reports a dope solution containing 0.08 kg cellulose fiber and 0.70 kg EMIMAc per 1 kg dope solution (Freire Ordóñez, Rozaria, et al., 2025 (Supplementary material)). In the present model, the cellulose fraction relative to cellulose and ionic liquid is:

$$\frac{0.00062}{0.00062 + 0.00755} = 0.0759 = 7.6\omega t\%$$

This is close to the 8 wt% cellulose level reported in the dope-solution inventory and supports the selected cellulose input as a realistic low-concentration cellulose/ionic-liquid formulation.

The activated carbon input was treated as a high-loading formulation assumption. The activated carbon fraction in the cellulose activated carbon solid phase is:

$$\frac{0.00193}{0.00193 + 0.00062} = 0.757 = 75.7\%$$

Cellulose activated carbon gels with activated carbon contents up to 70% of the total solids have been reported using dissolution regeneration processing. The value used here is slightly higher than that benchmark and was therefore retained as a high-loading activated carbon assumption supported by literature range and specialist consultation, not as a directly copied recipe. (Kim, 2025)

The shaping loss in the hydrogel route was calculated from the difference between the gelled material and the shaped actuator body:

$$0.0101\ kg - 0.00712\ kg = 0.00298\ kg$$

This corresponds to:

$$\frac{0.00298}{0.01010} * 100 = 29.5\%$$

This loss was treated as a production-stage shaping and trimming loss required to obtain the final actuator geometry and dimensions. It is not an end-of-life waste flow.

3.1.2.4 Inventory of Acrylic binder and selective coating

The acrylic binder was modeled using the Ecoinvent dataset “acrylic binder production, with water, in 54% solution state”. This dataset represents the production of 1 kg of acrylic binder containing 54 wt% binder in water and is used in Ecoinvent for acrylic paint production. The dataset includes raw materials, energy, infrastructure, land use, solid waste generation, and

emissions to air and water. (*Acrylic Binder Production, with Water, in 54% Solution State - Europe - Acrylic Binder, with Water, in 54% Solution State | EcoQuery*, n.d.)

In the actuator model, the acrylic binder was used as a structural binder/adhesive layer for electrode attachment and coating stabilization. The input amount was:

$$m_{binder,wet} = 0.00268\ kg = 2.68\ g$$

Because the dataset represents a 54% solution in water, the dry binder solid mass is:

$$m_{binder,dry} = 2.68\ g * 0.54 = 1.447\ g$$

The water fraction is:

$$m_{water} = 2.68\ g * 0.46 = 1.233\ g$$

The binder was assumed to be distributed over the same two-sided actuator surface as the selective coating. The two-sided area was calculated as:

$$0.120\ m * 0.024\ m * 2 = 0.00576\ m^2$$

$$0.00576\ m^2 = 57.6\ cm^2$$

Assuming a density close to water for the wet acrylic dispersion, the wet binder layer thickness is:

$$\frac{2.68\ cm^3}{57.6\ cm^2} = 0.0465\ cm = 0.465\ mm$$

For the dry acrylic solids:

$$\frac{1.447\ cm^3}{57.6\ cm^2} = 0.0251\ cm = 0.251\ mm$$

Therefore, the binder input was interpreted as a structural acrylic binder/adhesive layer rather than a thin electrochemical binder. The geometrical justification is shown in Table S5, and the scaled acrylic binder production inventory is provided in Table S6.

The selective coating was modeled using the Ecoinvent dataset “selective coat, copper sheet, sputter deposition”. This area-based process represents the coating of 1 m² copper sheet with chromium and tin oxide by sputtering and was used as a technological proxy for sputtering-based electrode/coating deposition. (*Selective Coating, Copper Sheet, Sputtering - Germany - Selective Coat, Copper Sheet, Sputter Deposition | EcoQuery*, n.d.)

The process was scaled to the two-sided actuator area:

$$A_{coating} = 0.00576\ m^2$$

The deposited coating mass was modeled separately as:

$$m_{coating} = 0.00020\ kg = 0.20\ g$$

This value can be obtained from an equivalent metallic coating layer of approximately 4 μm:

$$m = A * t * \rho$$

$$m = 0.00576\ m^2 * 4 * 10^{-6}\ m * 8700\ kg/m^3$$

$$m = 0.00020\ kg$$

The value of 0.00020 kg was therefore treated as an equivalent deposited electrode/coating-layer mass, not as the full copper-sheet substrate mass from the Ecoinvent dataset. The geometry and mass calculation are shown in Table S5, while the scaled selective coating inventory is provided in Table S7.

3.1.2.5 Inventory of the PDMS Actuator

The PDMS Actuator foreground inventory includes PDMS base, curing-agent proxy, auxiliary components, deposited selective coating, acrylic binder, methanol, deionized water, electricity, transport, waste plastic mixture, wastewater, methanol emission to water, and the final actuator output. The detailed stepwise foreground inventory for the PDMS actuator is provided in Table S8.

The PDMS mixture was modeled with:

$$m_{PDMS} = 0.00966\ kg$$

$$m_{curing\ agent} = 0.00097\ kg$$

The resulting ratio is:

$$\frac{0.00966}{0.00097} = 9.96$$

This is effectively a 10:1 base-to-curing-agent ratio. Dow describes SYLGARD 184 as a two-part, 10:1 silicone elastomer that can be cured at room temperature or accelerated by heat (Dow, 2017).

The exact curing agent dataset was unavailable. Therefore, a generic organic chemical proxy was used. This approach is consistent with the Delft thesis inventory for a PDMS microfluidic device, where “chemical, organic” was used as a proxy for the PDMS curing agent (Tjokro, 2023).

The main PDMS production loss occurs during replica removal and trimming:

$$0.01053\ kg - 0.00712\ kg = 0.00341\ kg$$

Together with the casting loss of 0.00010 kg, the total waste plastic mixture is:

$$0.00341\ kg + 0.0001\ kg = 0.00351\ kg$$

The trimming loss corresponds to:

$$\frac{0.00341}{0.01053} * 100 = 32.4\%$$

This was treated as a laboratory-scale casting and trimming loss caused by excess material required during molding, replica removal, and final shape formation. As with the hydrogel shaping loss, this is a production-stage loss rather than an end-of-life flow.

3.1.2.6 Electricity inventory and allocation

Electricity inputs were entered in OpenLCA as direct foreground flows assigned to the production of one actuator. Each electricity value was calculated from the operating power of representative laboratory equipment and the time required for the corresponding process step.

For the PDMS thermal steps, the Thermo Scientific Heratherm OGS60 oven was used as the reference device. This oven operates in the 50-250 °C range and consumes 194 W under controlled heating conditions. The oven is suitable for curing and drying operations at a laboratory scale (Thermo Scientific Heratherm Heating and Drying Ovens Efficient, Safe and Easy Thermoscientific, n.d.). The PDMS system was based on a SYLGARD 184-type formulation. SYLGARD 184 is a two-part silicone elastomer with a 10:1 base-to-curing-agent ratio and can be cured either at room temperature or by heat acceleration. The technical information gives heat-curing schedules such as 35 min at 100 °C, 20 min at 125 °C, and 10 min at 150 °C (Dow, 2017).

For the PDMS thermal curing step, the OpenLCA input was 0.120 kWh. Using the Heratherm OGS60 energy consumption, this corresponds to approximately 37 min of oven operation:

$$T = \frac{0.120\ kWh}{0.194\ kW} = 0.619\ h$$

$$0.619\ h * 60 = 37.1\ min$$

This operating time is consistent with the heat-curing time range reported for SYLGARD 184. Therefore, 0.120 kWh of electricity was used to cure one PDMS actuator.

For the post-curing/stabilization step, the OpenLCA input was 0.100 kWh. Using the same oven:

$$t = \frac{0.100\ kWh}{0.194\ kW} = 0.515\ h$$

$$0.515\ h * 60 = 30.9\ min$$

This value represents a short oven-based stabilization step after curing and before final testing. Therefore, 0.100 kWh of electricity was used for post-curing/stabilization of one PDMS actuator. For smaller operations, the Thermo Scientific Tube Revolver was used as the reference low-power laboratory device. The Tube Revolver has a maximum power of 6 W and is designed for mixing and rotation of laboratory samples (*Tube Revolver, Operation Manual 9240-11-021*, n.d.).

The 0.001 kWh values used for hydrogel regeneration and PDMS mixing correspond to 10 min of operation:

$$0.006\ kW * \frac{10}{60}\ h = 0.001\ kWh$$

The 0.0025 kWh values used for final quality control and functional testing correspond to 25 min of operation:

$$0.006\ kW * \frac{25}{60}\ h = 0.0025\ kWh$$

The 0.005 kWh value used for PDMS casting/shaping corresponds to 50 min of low-power auxiliary operation:

$$0.006\ kW * \frac{50}{60}\ h = 0.005\ kWh$$

The ionic liquid heating step was calculated from the amount of ionic liquid used in one actuator. The ionic liquid input was 0.00755 kg. The heat-capacity relation used was:

$$Q = mC_p\Delta T$$

For EmimOAc, the heat capacity was taken as 321.90 J mol^{-1} K^{-1}, and the molar mass is 170.21 g/mol, giving:

$$C_p = \frac{321.9}{0.17021} = 1.89\ kJ\ kg^{-1}K^{-1}$$

For a temperature increase of 75 K:

$$Q = 0.00755 * 1.89 * 75 = 1.07\ kJ$$

$$1.07\ kJ = 0.00030\ kWh$$

Including 25% heat loss for small-scale heating:

$$0.00030 * 1.25 = 0.000375\ kWh$$

$$0.000375\ kWh \approx 0.00038\ kWh$$

Thus, 0.00038 kWh of electricity was used to heat the ionic liquid in one hydrogel actuator. The heat-capacity equation and EmimOAc thermodynamic data are taken from the supporting LCI information for ionic liquids.

Table 6. Direct foreground electricity inputs and calculation basis

System	**Process**	**OpenLCA value**	**Calculation basis**	Explanation
Hydrogel	Heating of ionic liquid	0.00038 kWh	Heat required for 0.00755 kg IL + 25% heat loss	Small-scale ionic liquid heating
Hydrogel	Hydrogel regeneration	0.00100 kWh	6 W × 10 min	Low-power laboratory regeneration
Hydrogel	Final quality control	0.00250 kWh	6 W × 25 min	Low-power quality-control operation
PDMS	PDMS mixing	0.00100 kWh	6 W × 10 min	Low-power mixing operation
PDMS	Shaping	0.00500 kWh	6 W × 50 min	Low-power auxiliary shaping operation
PDMS	Thermal curing	0.12000 kWh	194 W oven × 37 min	Heat-curing of one PDMS actuator
PDMS	Stabilisation	0.10000 kWh	194 W oven × 31 min	Short oven stabilisation step
PDMS	Functional testing and finalisation	0.00250 kWh	6 W × 25 min	Low-power functional testing

Table 6 explains the foreground electricity inputs used in the OpenLCA model. The PDMS thermal steps were calculated based on the operating power of a Thermo Scientific Heraeus OGS60 oven. In contrast, small laboratory operations were calculated using the operating power of a Thermo Scientific Tube Revolver. The values are assigned to the production of one actuator.

3.1.2.7 Methanol cleaning inventory

Methanol was included as a minimal solvent input for surface cleaning of the PDMS actuator before the following processing steps. In laboratory PDMS preparation, volatile solvents are commonly used for surface cleaning or degreasing before bonding, coating, or further treatment. In this model, methanol was selected as a representative volatile cleaning solvent.

The methanol input was set to:

$$0.00020\ kg = 0.2\ g$$

Using a methanol density of approximately 0.7915 g/mL at 20 °C, this corresponds to:

$$\frac{0.2\ g}{\frac{0.7915\ g}{mL}} = 0.253\ mL$$

Therefore, the model takes approximately 0.25 mL of methanol per actuator. This amount was selected as the minimum practical quantity required for light wiping or degreasing of one actuator surface. It does not represent immersion cleaning, solvent bath cleaning, or repeated washing.

The full amount of methanol used for cleaning was included in the inventory as an emission flow to water:

$$0.0002\ kg$$

This conservative treatment ensures that the cleaning step is represented in the inventory and not excluded from the environmental assessment. The methanol calculation is summarised in Table S9.

3.1.2.8 Transport inventory

Transport was included for selected materials that were assumed to be delivered from Germany to the production location. Transport path of 1600 km was used for these delivered inputs. This represents a consolidated delivery scenario from a single supplier region rather than separate supplier-specific routes for each material.

Transport was calculated in OpenLCA in kg·km using the mass of the transported material:

$$Transport = mass * distance$$

For example, the ionic liquid input in the hydrogel model was 0.00755 kg. With a transport distance of 1600 km, the transport input becomes:

$$0.00755\ kg * 1600\ km = 12.08\ kg * km$$

The same calculation was applied to the other transported foreground materials. The full transport inventory is provided in Table S10.

The hydrogel coating related transport value of 4.928 kg·km corresponds to a transported mass of:

$$\frac{4.928\ kg * km}{1600\ km} = 0.00308\ kg$$

This mass includes the acrylic binder, deposited selective coating, and small coating related auxiliary material.

3.1.2.9 Waste, wastewater, and production losses

Waste and wastewater flows were included only when they were generated during actuator production. These flows represent production-stage losses, not the end-of-life treatment of the final actuator.

In the hydrogel route, wastewater is generated during precipitation, washing, purification, and phase separation/gelification. Each of these steps uses 0.010 kg of water. Assuming water density of 1000 kg/m³, this corresponds to:

$$\frac{\frac{0.010\ kg}{1000\ kg}}{m^3} = 1 * 10^{-5}\ m^3$$

Since four hydrogel water-processing steps were included, the total hydrogel wastewater flow was:

$$4 * 1 * 10^{-5} = 4 * 10^{-5}\ m^3$$

The hydrogel shaping step produced 0.00298 kg of inert waste. This value comes from the mass difference between the gelled material and the final shaped hydrogel body:

$$0.01010\ kg - 0.00712\ kg = 0.00298\ kg$$

This was modelled as shaping and trimming loss required to obtain the final actuator geometry.

In the PDMS route, plastic waste was generated during casting and trimming. The casting loss was 0.00010 kg, and the trimming loss was 0.00341 kg. Therefore, the total PDMS waste plastic mixture was:

$$0.00010\ kg + 0.00341\ kg = 0.00351\ kg$$

Wastewater in the PDMS route came from two cleaning steps using 0.001 kg of water each. This gives:

$$2 * \frac{0.001\ kg}{\frac{1000\ kg}{m^3}} = 2 * 10^{-6}\ m^3$$

Methanol used for PDMS cleaning was also included as an emission to water. The full methanol input of 0.00020 kg was assigned to this emission flow. The detailed waste, wastewater, and emission inventory is provided in Table S11.

3.1.2.10 Aggregated inventory comparison

The aggregated inventory highlights the main differences between the two actuator systems. The hydrogel route uses ionic liquid, cellulose, activated carbon, larger quantities of water, and produces shaping waste. The PDMS route uses PDMS, curing-agent proxy, methanol, higher direct electricity for curing and stabilization, and produces plastic waste during trimming.

Table 7 summarizes the main direct foreground flows for one 10 g Cellulosic Hydrogel Actuator and one 10 g PDMS Actuator. It includes the flows entered directly into the foreground model. In the full OpenLCA models, these foreground flows were linked to background providers, allowing upstream production, energy supply, transport, and treatment burdens to be included in the calculated results.

Table 7. Aggregated foreground inventory comparison for one 10 g actuator

Flow group	**Cellulosic Hydrogel Actuator**	**PDMS Actuator**	**Unit**
Final actuator mass	0.01	0.01	kg
Main material system	0.00755 ionic liquid + 0.00062 cellulose fibre	0.00966 PDMS + 0.00097 curing − agent proxy	kg
Activated carbon	0.00193	-	kg
Acrylic binder solution	0.00268	0.00268	kg
Deposited selective coating	0.0002	0.0002	kg
Methanol	-	0.0002	kg
Deionised/process water	0.04	0.002	kg
Direct foreground electricity	0.00388	0.2285	kWh
Foreground transport	21.09	21.936	$kg * km$
Main solid waste	0.00298 inert waste	0.00351 waste plastic mixture	kg
Wastewater	$4 * 10^{-5}$	$2 * 10^{-6}$	m^3
Methanol emission to water	-	0.0002	kg

In the PDMS system, thermal curing and stabilisation dominate direct electricity use:

$$0.120 + 0.1 = 0.220\ kWh$$

Relative to the total direct foreground electricity of 0.22850 kWh:

$$\frac{0.22}{0.2285} * 100 = 96.3\%$$

In other words, the majority of direct foreground electricity in the PDMS route is associated with thermal processing. In contrast, the hydrogel route has low direct electricity demand but higher water use and dependence on the upstream ionic liquid supply chain.

3.1.3 Life cycle impact assessment

The life cycle impact assessment (LCIA) stage was performed in OpenLCA using the Environmental Footprint (EF) v3.1 LCIA method. This method was selected because it provides a harmonized midpoint impact assessment framework for evaluating the life cycle environmental performance of products and organizations within the European Environmental Footprint approach. The same LCIA method was applied to both product systems, the Cellulosic Hydrogel Actuator and the PDMS Actuator, to maintain methodological consistency in the comparison. In the LCIA stage, the life cycle inventory flows from the two OpenLCA product systems were converted into environmental impact category indicators. This step is called characterization. Characterization links each relevant inventory flow to one or more environmental impact categories and converts it into a common category-specific unit. For example, greenhouse gas emissions are converted into climate change impacts expressed in kg CO_2 eq., while ozone-depleting substances are converted into ozone depletion impacts expressed in kg CFC-11 eq.

The EF v3.1 method includes 16 midpoint impact categories. These categories cover climate-related, toxicity-related, eutrophication-related, resource-related, water-related, and land-related environmental mechanisms. The categories, indicators, and units used in this study are shown in Table 8. The table is based on the EF v3.1 midpoint category structure reported by the Joint Research Center (JRC) (Bassi et al., 2023). Table 8 presents the EF v3.1 midpoint impact categories used for the LCIA calculation in OpenLCA. The same set of categories was applied to both actuator systems.

Table 8. EF v3.1 midpoint impact categories used in this study

Impact category	**Unit**
Climate change	kg CO_2 eq.
Ozone depletion	kg CFC-11 eq.
Human toxicity, cancer	CTUh
Human toxicity, non-cancer	CTUh
Particulate matter	Disease incidences
Ionizing radiation, human health	kBq U-235 eq.
Photochemical ozone formation, human health	kg NMVOC eq.
Acidification	mol H^+ eq.
Eutrophication, terrestrial	mol N eq.
Eutrophication, freshwater	kg P eq.
Eutrophication, marine	kg N eq.
Ecotoxicity, freshwater	CTUe
Land use	dimensionless
Water use	m^3 world eq. deprived water
Resource use, minerals and metals	kg Sb eq.
Resource use, fossils	MJ

The characterized EF v3.1 midpoint results were treated as the primary LCIA output in this thesis. They preserve the physical meaning and unit of each impact category and are therefore suitable for direct category-by-category comparison between the two actuator systems. All characterized results were calculated per functional unit, corresponding to the production of one 10 g actuator. In addition to characterized results, normalized EF v3.1 midpoint results were calculated. Normalization was applied because the characterized impact categories use different units and cannot be directly compared based on numerical magnitude alone. Normalization places the different categories on a common relative scale by dividing the characterized result of each category by a corresponding normalization factor:

$$Normalized\ result_i = \frac{Characterized\ result_i}{Normalization\ factor_i}$$

where i represents the impact category.

In the EF framework, normalization factors are based on reference inventory data and characterization factors. Joint Research Center (JRC) describe normalization as the step that converts characterized midpoint results into relative values using a reference inventory (Bassi et al., 2023). This allows comparison of the relative importance of different environmental categories within the same product system.

In this thesis, normalization was used only as a supporting interpretation tool. It was applied to express impact categories with different units on a common relative scale and to identify which categories were more important within the environmental profile of each actuator system. It was not used to replace the characterized results, and no weighted single-score result was used as the main comparison basis. The characterized EF v3.1 midpoint results remain the main quantitative basis for comparing the Cellulosic Hydrogel Actuator and the PDMS Actuator. The normalized results are used later to support hotspot identification and to help interpret the relative importance of impact categories.

The LCIA stage, therefore, produced two types of outputs:

- **Characterized EF v3.1 midpoint results**, used for the main category-by-category comparison.
- **Normalized EF v3.1 midpoint results**, used as an additional interpretive layer.

The interpretation procedure applied to these LCIA outputs is described in Section 3.1.4. The numerical results and their discussion are presented later in the Results and Discussion section.

3.1.4 Interpretation

The interpretation stage evaluated the inventory data and LCIA outputs obtained from the OpenLCA calculations. Here, the interpretation has been used as a structured methodological step rather than as an additional calculation method. The analysis assessed whether both actuator systems followed the same modeling logic. The model compared both systems using the same functional unit: the production of one actuator with a final mass of 10 g. It also applied the same cradle-to-gate, production-focused boundary to the Cellulosic Hydrogel Actuator and the PDMS Actuator. Both product systems used the same OpenLCA version, the Ecoinvent background database, the transport scenario, and the EF v3.1 LCIA method. This made the comparison consistent and ensured that the study evaluated two complete actuator production routes rather than isolated material quantities. The analysis examined the characterized EF v3.1 midpoint results category by category. Each midpoint category has its own unit and

environmental meaning, so the interpretation kept the categories separate rather than merging them into a single score. This approach helped identify which environmental pathways differed between the two actuator systems and preserved category-specific information. The hotspot analysis then identified the main contributors to the calculated impacts. In this thesis, a hotspot refers to any material input, process step, energy input, transport flow, waste flow, emission, or background process that contributes strongly to one or more EF v3.1 impact categories.

The interpretation also considered the normalized EF v3.1 results as a supporting analytical layer. Characterized midpoint categories use different units, so normalization helped place them on a common relative scale. However, the study did not use normalization to replace the characterized results or to create a final ranking. The study also did not use a weighted single score as the main basis for comparison. Instead, the characterized midpoint results remained the primary evidence, while the normalized results supported hotspot identification and showed the relative importance of different impact categories. Finally, the interpretation considered the main modeling assumptions and limitations, including the absence of ionic liquid recovery, the high activated carbon loading, the use of proxy datasets, treating shaping and trimming losses as production-stage waste, the methanol cleaning assumption, and the 1600 km transport scenario from Germany. These assumptions define the model's validity range and clarify how the results should be understood.

3.2 RESULTS

3.2.1 CHARACTERIZED EF V3.1 MIDPOINT RESULTS

The characterized EF v3.1 midpoint results demonstrate the environmental profiles of the Cellulosic Hydrogel Actuator and the PDMS Actuator for the production of one 10 g actuator which is the functional unit of this study. Figure 6 presents the full set of characterized indicators and subcategories in different reference units. Because the values span several orders of magnitude, the figure uses a logarithmic y-axis. This allows high-magnitude categories, such as freshwater ecotoxicity and land use, to be shown alongside very small toxicity- and ozone-related indicators in a single graph.

The overview figure is interpreted mainly as a within-category comparison between the two actuator systems. The indicators use different units, so bar heights across different categories should not be read as a direct ranking of environmental importance. Instead, Figure 6 shows

which actuator system has the highest result in each impact category and reveals the general direction of the comparison.

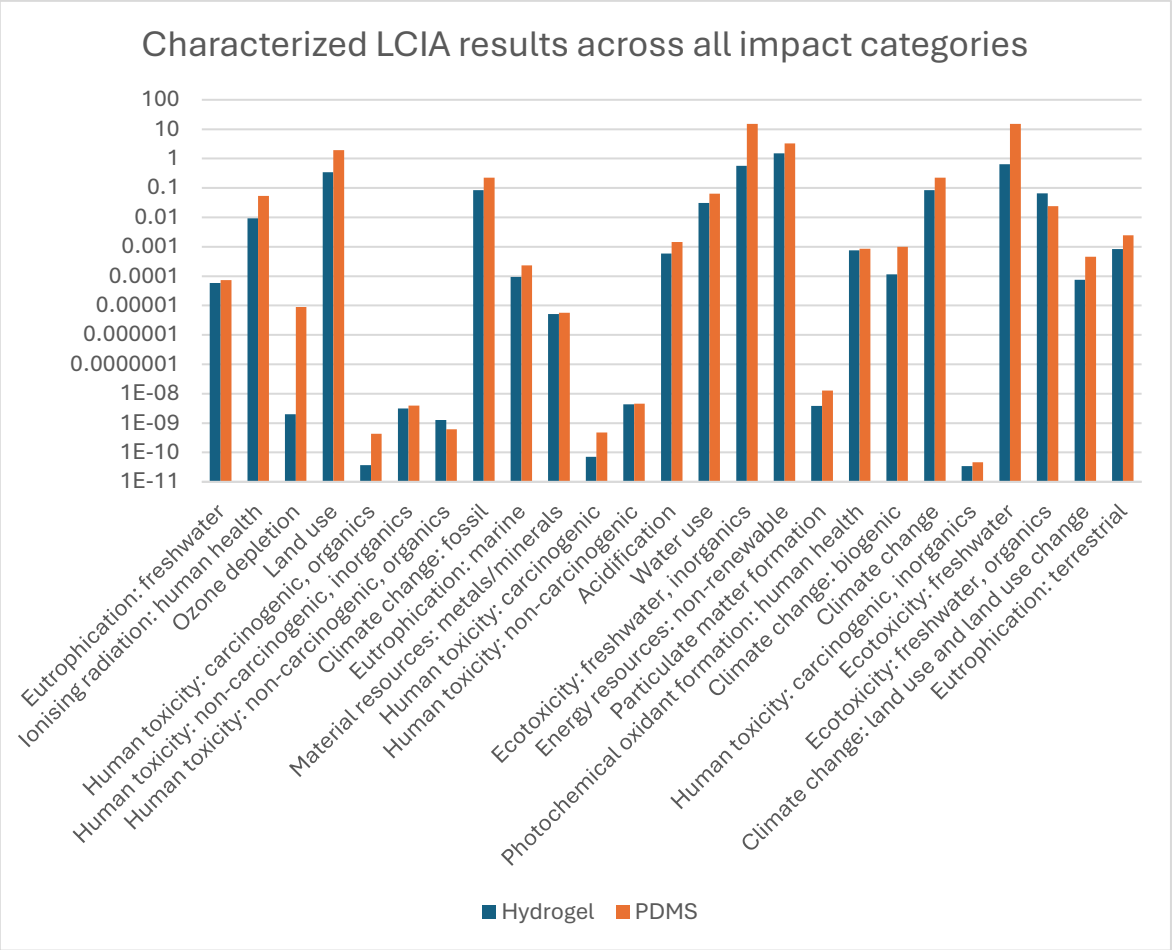

Eutrophication, freshwater (kg P-Eq)	Climate change categories (kg CO_2-Eq)	Freshwater ecotoxicity categories (CTUe)
Ionizing radiation, human health (kBq U235-Eq)	Eutrophication, marine (kg N-Eq)	Energy resources, non-renewable (MJ NCV)
Ozone depletion (kg CFC-11-Eq)	Material resources, metals/minerals (kg Sb-Eq)	Particulate matter formation (disease incidence)
Land use (dimensionless)	Acidification (mol H^+-Eq)	Photochemical oxidant formation, human health (kg NMVOC-Eq)
Human toxicity categories (CTUh)	Water use (m^3 world Eq deprived)	Eutrophication, terrestrial (mol N-Eq)

Figure 6. Characterized EF v3.1 midpoint results for the Cellulosic Hydrogel Actuator and the PDMS Actuator across all impact categories and subcategories, shown on a logarithmic scale.

The characterized results show a clear tendency toward higher potential environmental impacts for the PDMS Actuator across most assessed indicators. Of the 25 characterized indicators and subcategories shown in Figure 6, the PDMS Actuator has the highest result in 23, corresponding to 92% of the assessed indicators. The Hydrogel Actuator shows higher results only in two organic toxicity-related subcategories: human toxicity, organics, and freshwater ecotoxicity, organics. The largest relative differences occur in ozone depletion, freshwater ecotoxicity, land use, ionizing radiation, and carcinogenic toxicity, where the PDMS Actuator shows substantially higher impacts. This indicates that the Hydrogel Actuator has a lower environmental impact profile across most EF v3.1 midpoint categories, while the main trade-offs are concentrated in selected organic toxicity-related pathways. In Sections 3.2.1.1-3.2.1.7, the impact categories are grouped and discussed according to the type of environmental issue they represent.

3.2.1.1 Climate-related impacts

The climate-related indicators show a consistent difference between the two actuator systems. The PDMS Actuator shows higher results across the total climate change indicator and all three subcategories: fossil, biogenic, and land use and land-use change. These climate-related results are presented in Figure 7.

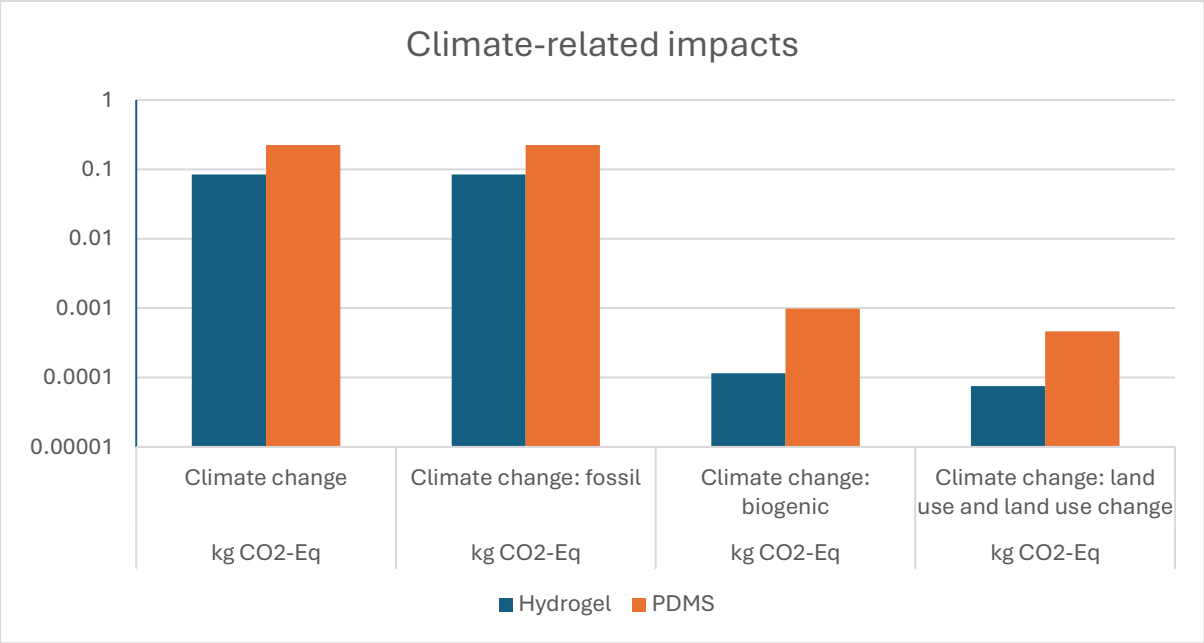

Figure 7. Characterized EF v3.1 midpoint results for climate-related impact categories, shown on a logarithmic scale

Total climate change results are 0.224 kg CO_2-Eq for PDMS and 0.0845 kg CO_2-Eq for Hydrogel, indicating that PDMS is approximately 2.66 times higher. The fossil climate change component follows almost the same ratio, with PDMS at 0.223 kg CO_2-Eq and Hydrogel at 0.0843 kg CO_2-Eq. This shows that fossil-related upstream processes dominate the climate change profile in both systems.

The biogenic and land-use-related climate components are smaller in absolute value but follow the same direction. PDMS is approximately 8.56 times higher in the biogenic climate component and 6.16 times higher in the land-use and land-use change component. These subcategories do not change the overall climate interpretation. Instead, they reinforce the conclusion that the PDMS route has the higher climate burden within the defined cradle-to-gate model.

3.2.1.2 Eutrophication and acidification impacts

The eutrophication and acidification indicators also show higher results for the PDMS Actuator across all categories. The characterized results for these impact categories are presented in Figure 8.

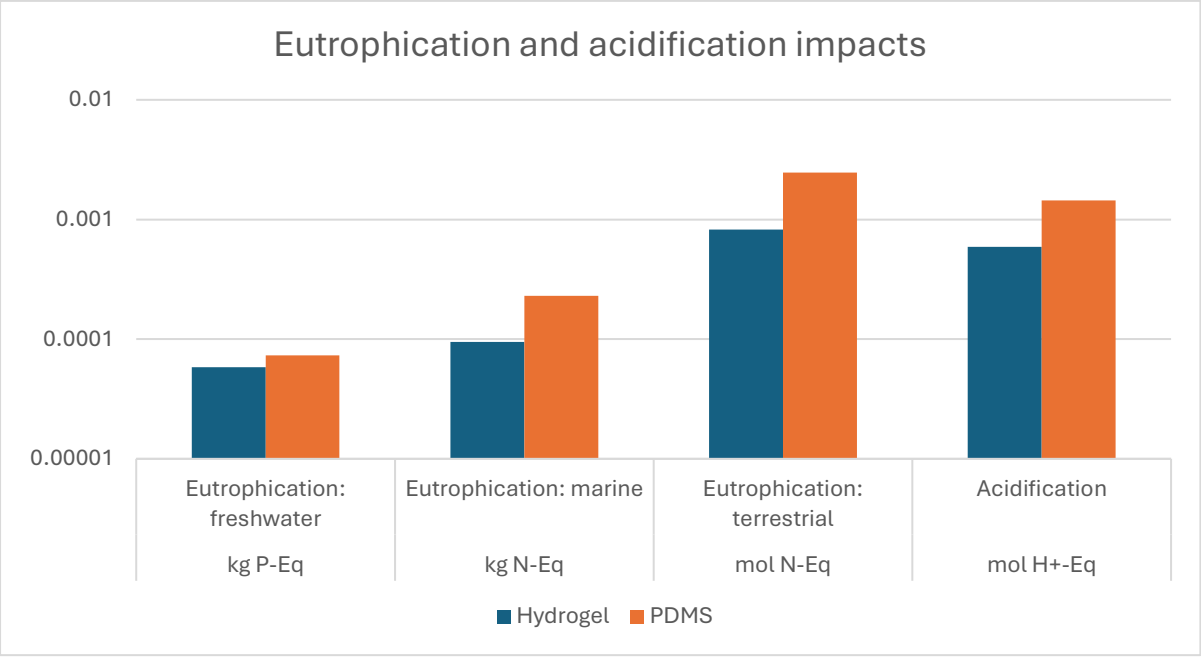

Figure 8. Characterized EF v3.1 midpoint results for eutrophication and acidification impact categories, shown on a logarithmic scale

The smallest difference appears in freshwater eutrophication, where PDMS is 1.26 times higher than Hydrogel. The gap becomes larger in marine eutrophication, where PDMS is 2.43 times

higher, and in terrestrial eutrophication, where PDMS is almost 3 times higher. Acidification follows the same pattern, with PDMS at 0.00145 mol H+-Eq and Hydrogel at 0.000591 mol H+-Eq, corresponding to a 2.45-fold increase.

These results indicate that the PDMS system imposes a higher burden across several nutrient- and acidification-related pathways rather than in a single isolated category. The smaller difference in freshwater eutrophication also shows that the advantage of Hydrogel is not equally strong across all ecosystem-related indicators.

3.2.1.3 Air pollution-related impacts

The air pollution-related group includes photochemical ozone formation, which affects human health, and particulate matter formation. Both indicators are higher for the PDMS Actuator, but the strength of the difference differs substantially. The characterized results for these air pollution-related indicators are presented in Figure 9.

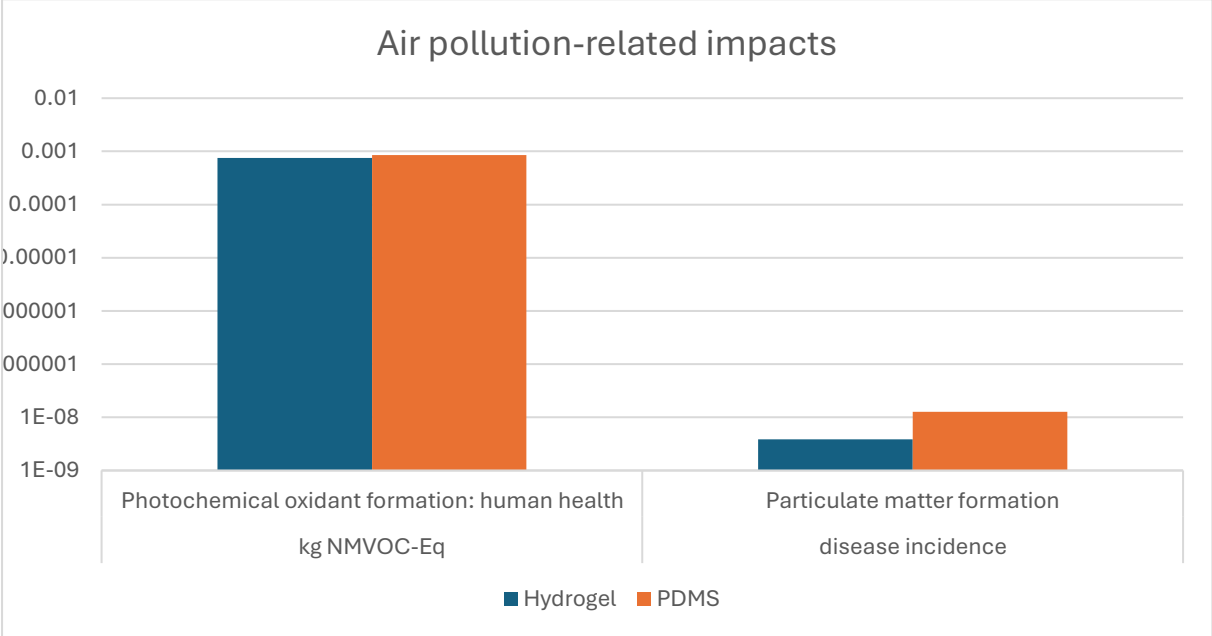

Figure 9. Characterized EF v3.1 midpoint results for air pollution-related impact categories, shown on a logarithmic scale.

Photochemical ozone formation is one of the closest categories in the comparison. PDMS Actuator reaches $8.58 * 10^{-4}$ kg NMVOC-Eq, while the Hydrogel Actuator reaches $7.57 * 10^{-4}$ kg NMVOC-Eq, making PDMS results only 1.13 times higher. By contrast, particulate matter formation shows a clearer separation. PDMS Actuator reaches $1.27 * 10^{-8}$ disease

incidence, compared with $3.84 * 10^{-9}$ for the Hydrogel Actuator, resulting in a PDMS value approximately 3.29 times higher.

This means the air pollution-related profile does not differ equally across both pathways. The difference is small for photochemical ozone formation, but more pronounced for particulate matter formation.

3.2.1.4 Human toxicity impacts

The human toxicity results show a more complex pattern than the climate, eutrophication, acidification, and air-related categories. The carcinogenic indicators are consistently higher for PDMS, while the non-carcinogenic profile contains one of the main trade-offs in the study. The characterized results for the human toxicity indicators are presented in Figure 10.

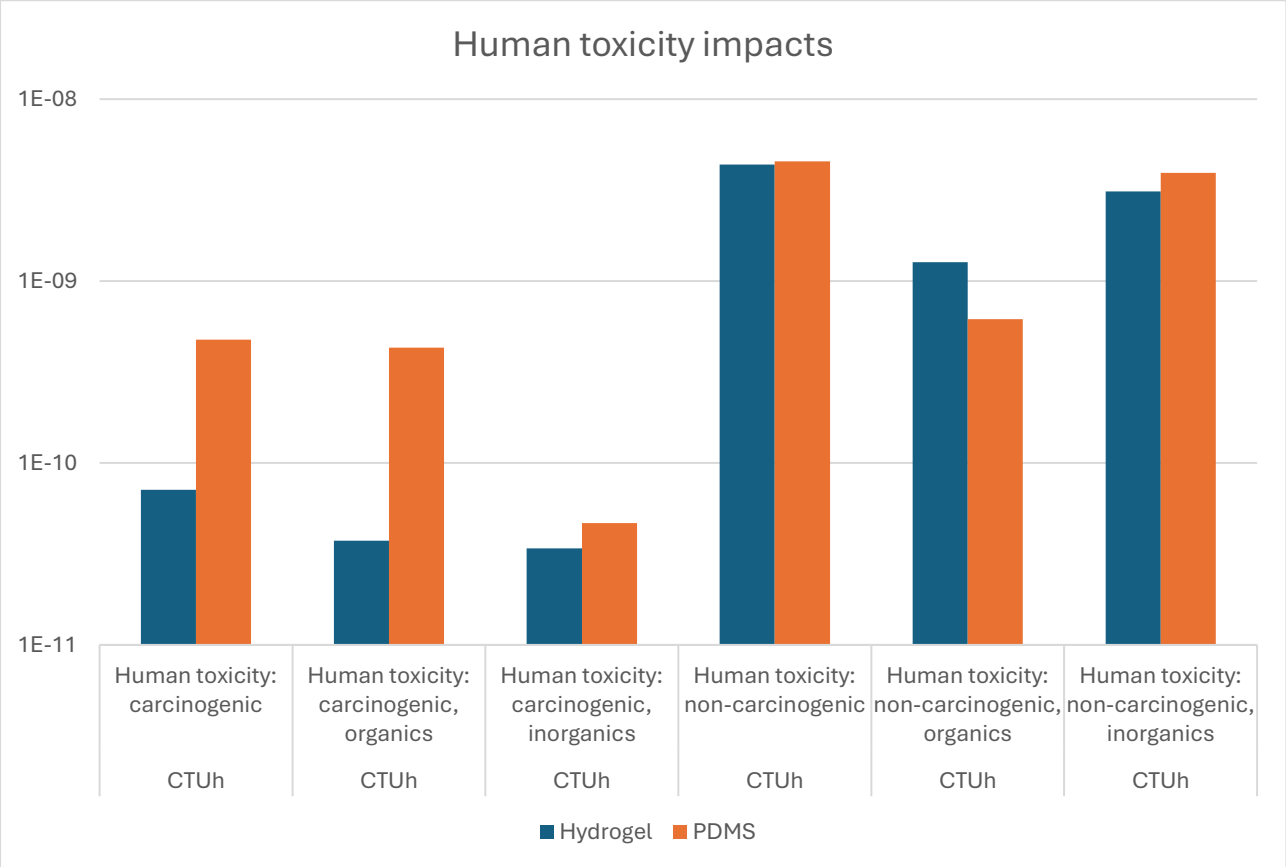

Figure 10. Characterized EF v3.1 midpoint results for human toxicity impact categories, shown on a logarithmic scale.

The aggregated carcinogenic toxicity result is $4.76 * 10^{-10}$ CTUh for PDMS and $7.14 * 10^{-11}$ CTUh for Hydrogel. This makes PDMS approximately 6.68 times higher. The organic carcinogenic subcategory shows a larger difference, with PDMS approximately 11.5 times

higher than Hydrogel. The inorganic carcinogenic subcategory follows the same direction, although the difference is smaller, with PDMS approximately 1.37 times higher.

The non-carcinogenic toxicity profile is more balanced. The aggregated non-carcinogenic indicator is almost equal between the two systems: $4.55 * 10^{-9}$ CTUh for PDMS and $4.38 * 10^{-9}$ CTUh for Hydrogel. This corresponds to only a 1.04 fold difference. However, the subcategories reveal opposing tendencies. PDMS is higher in the inorganic fraction, while Hydrogel is 2.06 times higher in the organic fraction. That shows that the near-equal aggregated non-carcinogenic result does not come from identical profiles, but from opposing contributions within the subcategories.

3.2.1.5 Freshwater ecotoxicity impacts

Freshwater ecotoxicity shows one of the clearest overall differences between the two actuator systems. The aggregated freshwater ecotoxicity result is much higher for PDMS, although the organic subcategory shows a trade-off in the opposite direction. The characterized results for the freshwater ecotoxicity indicators are presented in Figure 11.

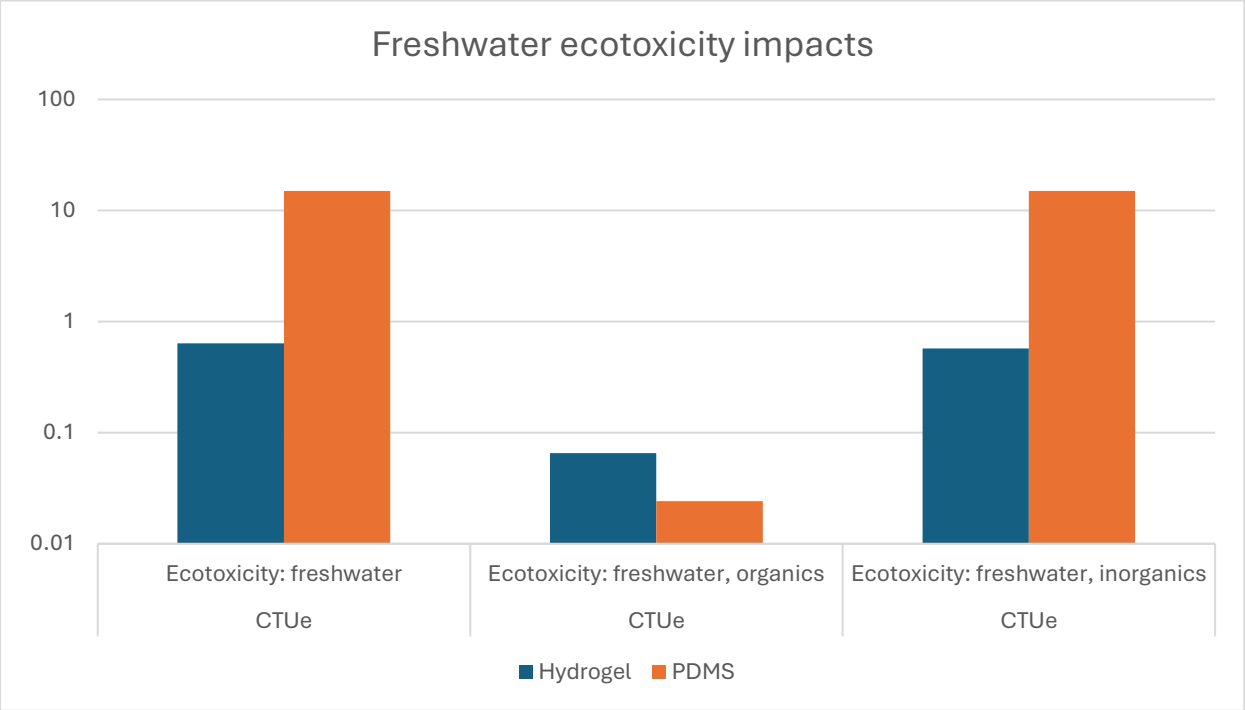

Figure 11. Characterized EF v3.1 midpoint results for freshwater ecotoxicity impact categories, shown on a logarithmic scale.

The total freshwater ecotoxicity result is 15.01 CTUe for PDMS and 0.638 CTUe for Hydrogel. This means that PDMS is approximately 23.5 times higher. The inorganic component is the

main driver of this difference: PDMS reaches 14.98 CTUe, while Hydrogel reaches 0.573 CTUe, giving a ratio of approximately 26.2.

The organic ecotoxicity subcategory shows the opposite pattern. Hydrogel reaches 0.0655 CTUe, while PDMS reaches 0.0242 CTUe, meaning that Hydrogel is approximately 2.70 times higher in this specific subcategory. However, the inorganic component dominates the aggregated ecotoxicity result, so the total freshwater ecotoxicity profile remains clearly less favorable for PDMS.

3.2.1.6 Resource use impacts

The resource use group includes non-renewable energy resources, mineral and metal resources, water use, and land use. PDMS has higher results in all four categories. The characterized results for the resource use indicators are presented in Figure 12.

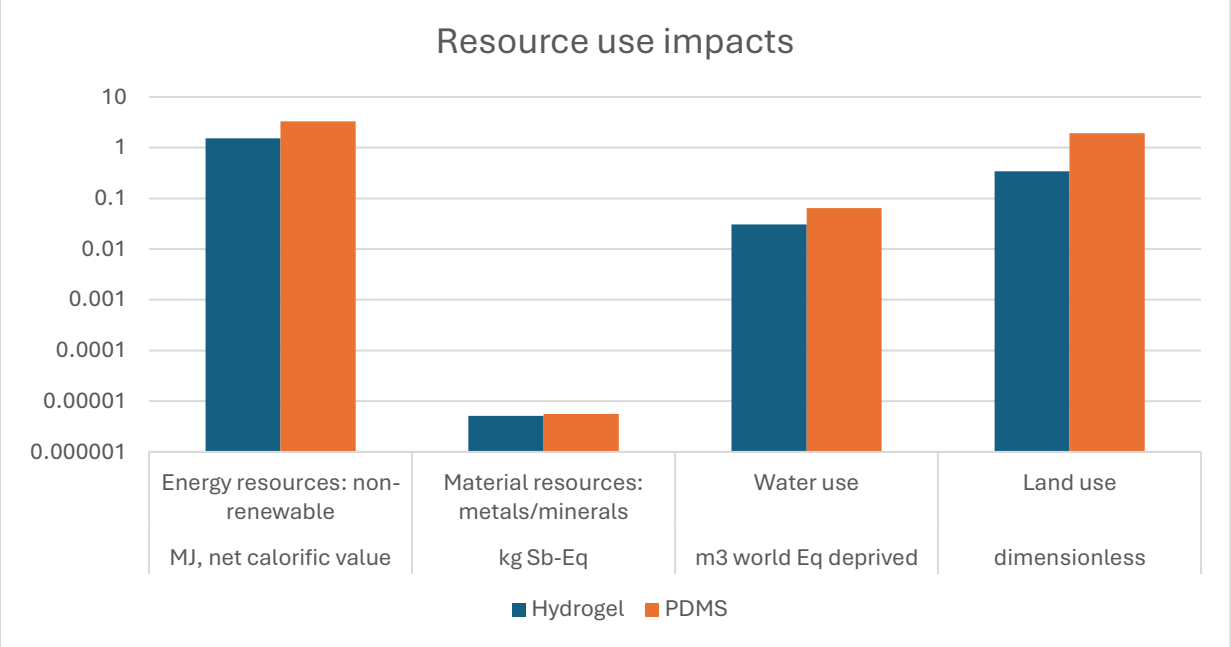

Figure 12. Characterized EF v3.1 midpoint results for resource use impact categories, shown on a logarithmic scale.

For non-renewable energy resources, PDMS reaches 3.31 MJ, while Hydrogel reaches 1.52 MJ. This makes PDMS approximately 2.18 times higher. Water use follows a similar pattern, with PDMS at 0.0640 m^3 world Eq deprived and Hydrogel at 0.0305 m^3 world Eq deprived, resulting in a 2.10-fold difference. This result is important because the Hydrogel route includes several water-based preparation and purification steps, yet it does not exceed PDMS in the EF v3.1 water use indicator.

The biggest difference in this group appears in land use. PDMS reaches 1.92, while Hydrogel reaches 0.341, making PDMS approximately 5.63 times higher. By contrast, the two systems are close in material resources: metals/minerals. PDMS is only 1.09 times higher than Hydrogel in this category. This indicates that the resource-related advantage of Hydrogel is stronger for energy, water, and land use than for mineral and metal resource depletion.

3.2.1.7 Ozone depletion and ionising radiation impacts

Ozone depletion and ionizing radiation were grouped as specific impact categories outside the broader thematic groups. Both indicators show higher results for the PDMS Actuator. The characterized results for ozone depletion and ionising radiation are presented in Figure 13.

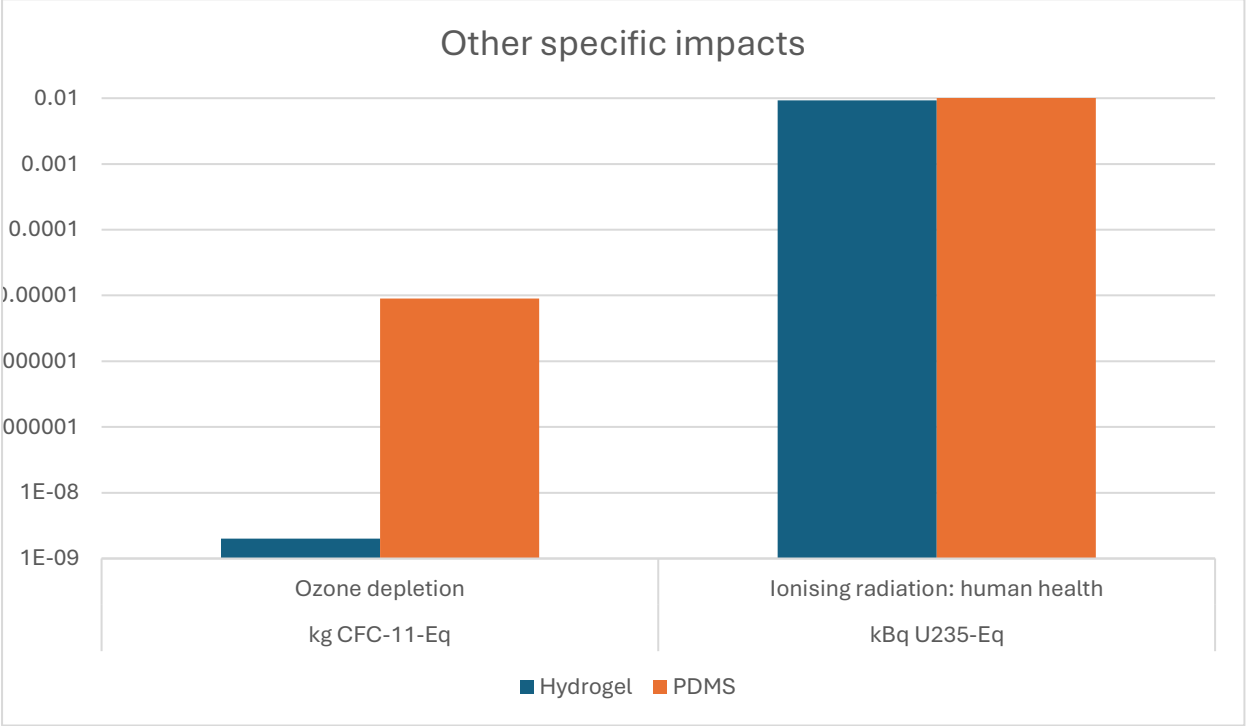

Figure 13. Characterized EF v3.1 midpoint results for ozone depletion and ionizing radiation, shown on a logarithmic scale.

Ozone depletion shows the largest relative difference in the entire characterized comparison. PDMS reaches $9 * 10^{-6}$ kg CFC-11-Eq, while Hydrogel reaches $2.01 * 10^{-9}$ kg CFC-11-Eq. This makes the PDMS result approximately 4478 times higher. Because of the very small Hydrogel value, this category produces an extremely large ratio and represents one of the strongest hotspots for the PDMS system.

Ionizing radiation follows the same direction but with a less extreme difference. PDMS reaches 0.0542 kBq U235-Eq, compared with 0.00931 kBq U235-Eq for Hydrogel. This means that PDMS is approximately 5.82 times higher. Together, these two indicators reinforce the broader pattern in which PDMS shows a heavier environmental profile in most EF v3.1 midpoint categories.

3.2.2 NORMALIZED EF V3.1 MIDPOINT RESULTS

The normalized EF v3.1 results for the Cellulosic Hydrogel Actuator and the PDMS Actuator, presented in Figure 14, were used to support the interpretation of relative category importance within the environmental performance of the two actuator systems. Normalization does not replace the characterized midpoint results. Instead, it places categories with different units on a common relative scale. Which helps to identify which impact categories contribute most strongly to the environmental profile of each actuator system.

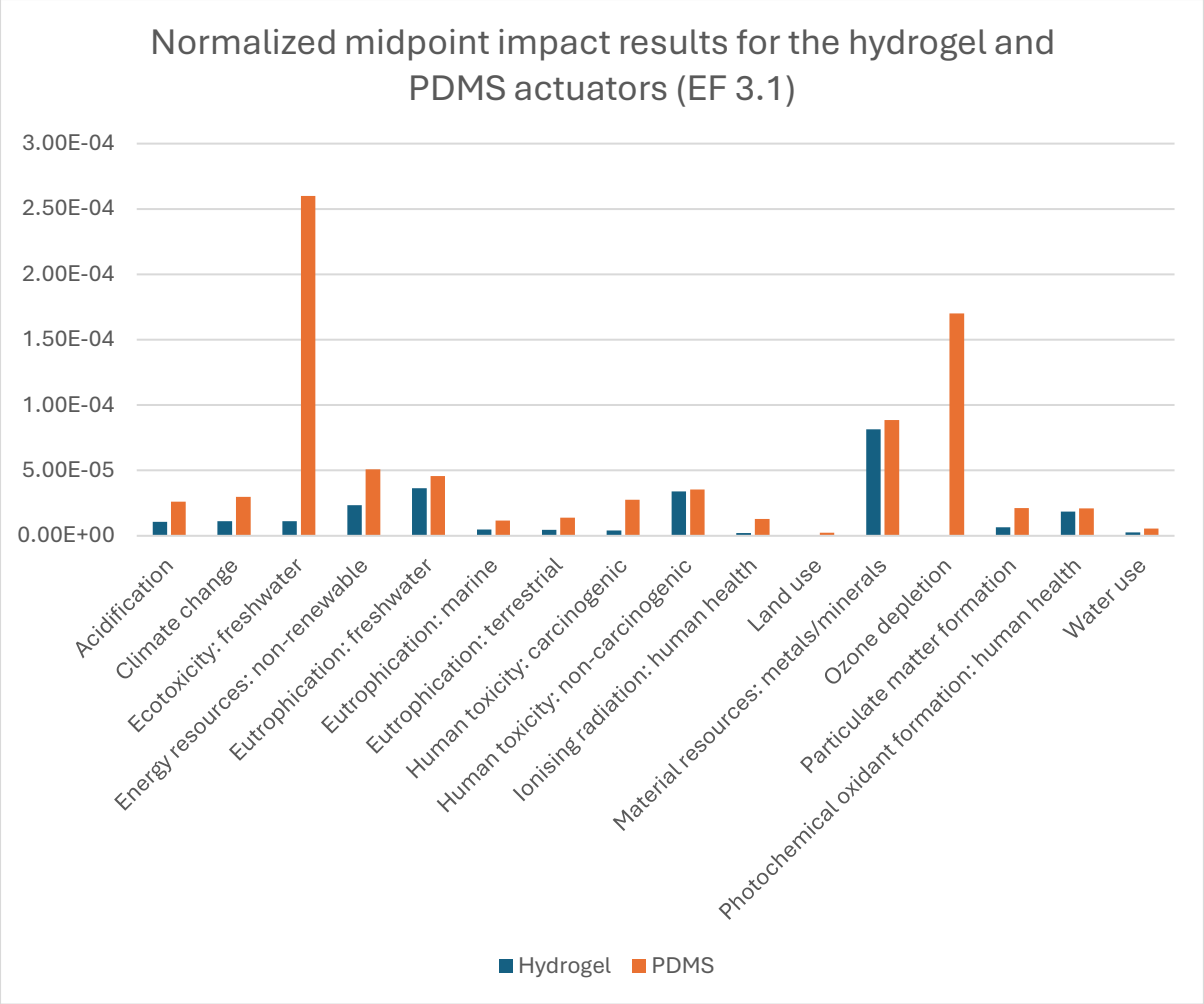

Figure 14. Normalized EF v3.1 midpoint results for the Cellulosic Hydrogel Actuator and the PDMS Actuator. Normalized values are dimensionless and represent characterized results divided by EF v3.1 normalization factors.

The normalized results follow the same pattern as the characterized results. The PDMS Actuator has higher scores in most impact categories, while the Hydrogel Actuator remains lower in most of them. The biggest normalized differences are seen in freshwater ecotoxicity and ozone depletion. Clear differences are also visible in climate change, acidification, particulate matter formation, ionizing radiation, freshwater eutrophication, and non-renewable energy use.

The normalized profile also shows that the difference between the two systems is not equally big across all categories. The gap is smaller in material resources: metals/minerals, photochemical ozone formation, human toxicity: non-carcinogenic, and water use. These categories indicate that the Hydrogel Actuator does not outperform PDMS by the same margin across all environmental pathways.

Within the Hydrogel system, the normalized profile fells more distributed across several categories, especially material resources, freshwater eutrophication, non-carcinogenic human toxicity, and non-renewable energy resources. In contrast, the PDMS profile is more concentrated, with freshwater ecotoxicity and ozone depletion standing out as dominant hotspots. This means that PDMS is not only higher in many categories but also concentrates a substantial share of its environmental burden in a smaller number of highly pronounced impact pathways.

3.3 DISCUSSION

3.3.1 Environmental interpretation of the actuator systems in the global context

This thesis compared two routes for soft robotic actuators by modeling the cradle-to-gate production of one 10 g Cellulosic Hydrogel Actuator and one 10 g PDMS Actuator. Both systems were assessed with the same functional unit, system boundary, background database, and EF v3.1 midpoint method. This made the comparison consistent and allowed the two actuator routes to be evaluated as complete production systems rather than as isolated materials. The characterized results showed greater impacts for the PDMS Actuator across most categories, while the Hydrogel Actuator generally had a lower environmental profile. The normalized results provide another perspective on this comparison. Instead of only showing which actuator has the higher result in each category, normalization relates the impacts to global reference impact values per person. That helps to identify which specific categories are more relevant in a broader environmental context and avoids simply repeating the characterized midpoint results (Bassi et al., 2023).

In this study, the production of a single 10 g actuator accounted for only a small fraction of the corresponding global per-person reference value in each category. The highest normalized result for PDMS was freshwater ecotoxicity, with a value of $2.6 * 10^{-4}$, corresponding to about 0.026% of the reference value. The next-highest normalized result was ozone depletion, with a value of $1.7 * 10^{-4}$, or about 0.017%. For Hydrogel, the highest normalized result was material resources: metals/minerals, with $8.14 * 10^{-5}$, or about 0.0081%. These values show that a single laboratory-scale actuator does not represent a significant environmental burden relative to global per-person impacts. However, this should not be interpreted as a final industrial footprint. Both systems were modeled as laboratory-scale routes for emerging

actuator materials. Therefore, the normalized values are more useful as early-stage comparative indicators, as they show where the main environmental concerns occur in current production routes.

The PDMS Actuator had not only higher-characterized impacts across most categories, but also a more concentrated normalized profile. Freshwater ecotoxicity and ozone depletion were the clearest normalized hotspots for PDMS. Climate change was also greater for PDMS than for Hydrogel. Still, its normalized value of $2.97 * 10^{-5}$ was lower than those for freshwater ecotoxicity, ozone depletion, material resources, and non-renewable energy use. Therefore, the PDMS route should not be discussed only in terms of carbon footprint. In the EF normalization context, toxicity- and ozone-related pathways are more important for understanding its relative environmental burden. PDMS is still widely used in soft robotics due to its properties for different actuator designs (S. Li et al., 2023; Miranda et al., 2022). But, these technical advantages do not automatically mean lower environmental impact.

The Hydrogel Actuator showed a different pattern. Its normalized impacts were generally lower and more evenly distributed across several categories, including material resources, freshwater eutrophication, non-carcinogenic human toxicity, non-renewable energy resources, and photochemical ozone formation. This means that the hydrogel route did not show a single dominant hotspot, unlike the PDMS results for freshwater ecotoxicity and ozone depletion. Still, the Hydrogel should not be described as automatically sustainable only because it contains cellulose. Cellulose-based hydrogels are often considered promising soft robotic materials due to their renewable origin, water-rich structure, softness, and relevance to bioinspired systems (Kundu et al., 2022; Nasseri et al., 2023; Park et al., 2024). In the present model, however, the Hydrogel Actuator also required ionic liquid, activated carbon, acrylic binder, selective coating materials, water-based processing, and wastewater treatment. No ionic liquid recovery was included. This is an important limitation because [EMIM][OAc] was treated as consumed or lost during preparation. As a result, the hydrogel scenario may be conservative compared to a future process in which part of the ionic liquid is recovered and reused. At the same time, it would also be uncertain to assume recovery without measured data, because recovery may require additional heat, electricity, separation, evaporation, or purification. The high activated carbon loading and the use of proxy datasets also limit the models precision. So the hydrogel result should be read as a conservative laboratory-scale production scenario, not as a fully optimized hydrogel process. This interpretation aligns with

studies showing that ionic-liquid-based cellulose processing can be strongly influenced by ionic-liquid production, electricity demand, and recovery-related processing (Freire Ordóñez, Pontillo, et al., 2025; Szabó et al., 2023).

The comparison also shows that the difference between the systems is not absolute. Material resources: metals/minerals were close, with $8.14 * 10^{-5}$ for Hydrogel and $8.84 * 10^{-5}$ for PDMS. Human toxicity: non-carcinogenic was also close, with $3.4 * 10^{-5}$ for Hydrogel and $3.54 * 10^{-5}$ for PDMS. These similarities are partly due to shared auxiliary inputs, acrylic binders and selective coating materials. They also introduce uncertainty because the binder and coating were represented using available datasets and proxies. The PDMS route also included a simplified methanol cleaning assumption, and both systems used a fixed foreground transport scenario. Replacing the main actuator matrix does not remove all environmental burdens from the system. The actuator should be understood as a full material-processing route, not only as a choice between cellulose and PDMS.

3.3.2 Future research

Future research should build directly on this model's limitations. The first important step is to improve the hydrogel inventory, especially the treatment of [EMIM][OAc]. In this thesis, no ionic liquid recovery was modeled, so the hydrogel route was treated as if the ionic liquid was consumed or lost during laboratory-scale preparation. A future study should test this assumption more carefully. Recovery may reduce the need for new ionic liquid production, but it should not be assumed to automatically improve the environmental profile. It may also require additional heat, electricity, membrane separation, evaporation, purification, or other processing steps. Therefore, future work should compare no-recovery, partial-recovery, and high-recovery scenarios using measured recovery efficiencies and measured process energy demand. This would show whether the hydrogel route is mainly affected by ionic liquid production itself or by the additional recovery process needed to make the route more circular.

A second direction is to shift from a mass-based to a performance-based functional unit. The current comparison based on a single 10 g actuator is suitable for early-stage production modeling, but soft robotic actuators are functional components, not just material samples. Future comparisons should include actuator performance and service lifetime. This could change the interpretation if one actuator has a lower production impact but shorter lifetime, lower force output, slower response, or higher maintenance needs. PDMS may offer practical advantages for dry-state handling, though its mechanical properties can change over time and

should be measured for the specific actuator system. Hydrogels, by comparison, may require hydration management and may exhibit property changes during use (Park et al., 2024; Y. Zhang, Adam, et al., 2024). Therefore, future LCA work should normalize environmental impacts according to useful actuation output rather than using mass-based functional units.

Once more reliable data become available, the system boundary should be extended beyond the cradle-to-gate stage to reflect a more complete life-cycle perspective. This would allow future studies to account not only for material production but also for the use phase, including energy demand, hydration or storage conditions, maintenance needs, replacement frequency, and end-of-life options such as recycling, biodegradation, or disposal. For PDMS-based actuators, particular attention should be given to the treatment of crosslinked silicone elastomers and waste generated during plastic production. For the cellulose-based hydrogel route, future work should further investigate biodegradation behavior, potential ionic liquid residues, electrode separation, coating removal, and the treatment of composite hydrogel waste.

Finally, future studies should place more emphasis on the role of auxiliary materials. In some normalized resource- and toxicity-related impact categories, the results for the hydrogel and PDMS systems were relatively close. This was partly because both systems relied on similar supporting materials, such as acrylic binder and selective coatings. Therefore, improving the main actuator material alone is unlikely to be sufficient. Future scenarios should also consider the broader material and process system, including alternative electrode systems, lower-mass conductive layers, bio-based binders, carbon-based coatings, reusable substrates, renewable electricity, batch processing, and reduced trimming losses. This would allow the assessment to move beyond a direct comparison of two laboratory-scale routes and provide more practical guidance for the development of sustainable soft robotic actuator systems.

3.3.3 Conclusions

Overall, the results suggest that the cellulose-based hydrogel actuator had a lower cradle-to-gate environmental profile than the PDMS actuator within the assumptions of this laboratory-scale model. However, this does not mean that hydrogel actuators are automatically sustainable. The hydrogel route cannot be treated as impact-free, even though it performed better overall. Its environmental burden is linked to the use of ionic liquid processing, the addition of activated carbon, the need for binder and coating layers, and the wastewater produced during fabrication. The PDMS route showed higher impacts in most EF v3.1 midpoint categories. The clearest concerns for this system were freshwater ecotoxicity and

ozone depletion. Future improvements should therefore focus on the whole actuator system rather than only on the main material. This includes better solvent recovery, improved electrode and coating design, more efficient processing, and functional units based on actuator performance rather than mass alone.

SUMMARY

Soft robotic actuators are usually introduced through their movement, flexibility, response to stimuli, and role in bioinspired systems. In this thesis, they are considered from a different angle: as material systems with an environmental burden already at the production stage. A soft actuator is not only a functional moving part; it also brings together raw materials, solvents, coatings, electricity, water, transport, wastewater, and production waste. The study compared a cellulose-based hydrogel actuator with a polydimethylsiloxane (PDMS) actuator to see whether the hydrogel route can be a more environmentally favorable alternative to the conventional silicone-based route. A cradle-to-gate LCA was carried out for one 10 g actuator in OpenLCA, using Ecoinvent 3.11 and the EF v3.1 midpoint method. The model covered raw material and precursor production, laboratory fabrication, selected transport, energy and water consumption, ancillaries, coatings, solvent use, wastewater, and process waste. The use phase and end-of-life were left outside the system boundary because comparable data on lifetime, actuation cycles, degradation, maintenance, and disposal were not available for these laboratory-scale systems.

The hydrogel actuator had lower impacts in most of the assessed categories. In climate change, the PDMS route reached 0.224 kg CO_2-eq per actuator, while the hydrogel route reached 0.0845 kg CO_2-eq, so the PDMS result was about 2.66 times higher. PDMS also had higher values for acidification, eutrophication, land use, water use, non-renewable energy use, ozone depletion, and freshwater ecotoxicity. The largest contrast appeared in freshwater ecotoxicity, where PDMS reached 15.01 CTUe, and the hydrogel actuator reached 0.638 CTUe. The normalized results showed the same general trend: the PDMS profile was particularly notable for freshwater ecotoxicity and ozone depletion. However, the hydrogel route cannot be considered automatically sustainable. Its impact was still associated with the use of ionic liquid, activated carbon, acrylic binder, selective coating materials, water treatment, and wastewater treatment. Since the model is based on laboratory-scale data, proxy datasets, and equal actuator mass, it should be understood as an early production-stage comparison. Future LCA studies could be made more comprehensive by using measured process data, considering ionic liquid recovery scenarios, alternative electrode and coating systems, renewable energy, improved processing conditions, and a functional unit related to actuator operation rather than just its mass.

REFERENCES

AboZaid, Y. A., Aboelrayat, M. T., Fahim, I. S., & Radwan, A. G. (2024). Soft robotic grippers: A review on technologies, materials, and applications. In *Sensors and Actuators A: Physical* (Vol. 372). Elsevier B.V. https://doi.org/10.1016/j.sna.2024.115380

acrylic binder production, with water, in 54% solution state - Europe - acrylic binder, with water, in 54% solution state | ecoQuery. (n.d.). Retrieved May 3, 2026, from https://ecoquery.ecoinvent.org/3.12/cutoff/dataset/2973/documentation

Ahmed, E. M. (2015). Hydrogel: Preparation, characterization, and applications: A review. In *Journal of Advanced Research* (Vol. 6, Number 2, pp. 105–121). Elsevier B.V. https://doi.org/10.1016/j.jare.2013.07.006

Ariati, R., Souza, A., Souza, M., Zille, A., Soares, D., Lima, R., & Ribeiro, J. (2024). Mechanical and optical properties assessment of an innovative PDMS/beeswax composite for a wide range of applications. *Journal of the Mechanical Behavior of Biomedical Materials*, *160*. https://doi.org/10.1016/j.jmbbm.2024.106716

Bassi, A., Biganzoli, S., Ferrara, F., Amadei, N., Valente, A., Sala, A., & Ardente, S. (2023). *Updated characterisation and normalisation factors for the Environmental Footprint 3.1 method*. https://doi.org/10.2760/798894

Chen, J., Cao, Y., Pei, J., & Zhao, H. (n.d.). *Supporting Information A Multifunctional Actuator Based on Graphene/PDMS Composite Material with Shape Programmable Configuration and High Photothermal Conversion Capability*.

Chen, J., Cao, Y., Pei, J., & Zhao, H. (2023). Multifunctional Actuator Based on Graphene/PDMS Composite Materials with Shape Programmable Configuration and High Photothermal Conversion Capability. *ACS Applied Materials and Interfaces*, *15*(26), 31917–31926. https://doi.org/10.1021/acsami.3c06041

Dong, X., Wang, C., Song, H., Shao, J., Lan, G., Zhang, J., Li, X., & Li, M. (2024). Advancement in Soft Hydrogel Grippers: Comprehensive Insights into Materials, Fabrication Strategies, Grasping Mechanism, and Applications. In *Biomimetics* (Vol. 9, Number 10). Multidisciplinary Digital Publishing Institute (MDPI). https://doi.org/10.3390/biomimetics9100585

Dow. (2017). *SYLGARD^{TM} 184 Silicone Elastomer Technical Data Sheet*.

El-Atab, N., Mishra, R. B., Al-Modaf, F., Joharji, L., Alsharif, A. A., Alamoudi, H., Diaz, M., Qaiser, N., & Hussain, M. M. (2020). Soft Actuators for Soft Robotic Applications: A Review. *Advanced Intelligent Systems*, *2*(10). https://doi.org/10.1002/aisy.202000128

Eyvazian, A., Song, Y., Hovhannes, C., Savari, A., & Sawaran Singh, N. S. (2026). State-of-the-art soft robotic systems for unstructured and real-world environments: A systematic review. *Engineering Science and Technology, an International Journal*, *73*, 102264. https://doi.org/10.1016/j.jestch.2025.102264

Freire Ordóñez, D., Pontillo, A. R. N., Mac Dowell, N., Welton, T., & Lee, K. Y. (2025). Unveiling the environmental costs of lignocellulosic film production with ionic liquids: the case of 1-ethyl-3-methylimidazolium acetate. *RSC Sustainability*, *3*(7), 3002–3008. https://doi.org/10.1039/d5su00212e

Freire Ordóñez, D., Rozaria, A., Pontillo, N., Dowell, N. Mac, Welton, T., & Lee, K.-Y. (2025). *Supplementary material to "Unveiling the environmental costs of lignocellulosic film production with ionic liquids: The case of 1-ethyl-3-methylimidazolium acetate."*

Hassan, E.-S. R. E., & Mutelet, F. (2017). Use of Ionic Liquids for the Treatment of Biomass Materials and Biofuel Production. In *Carbohydrate*. InTech. https://doi.org/10.5772/67026

International Organization for Standardization. (2006a). *ISO 14040:2006 Environmental management — Life cycle assessment — Principles and framework*.

International Organization for Standardization. (2006b). *ISO 14044:2006 Environmental management — Life cycle assessment — Requirements and guidelines*.

Katzer, K., Kanan, A., Pfeil, S., Grellmann, H., Gerlach, G., Kaliske, M., Cherif, C., & Zimmermann, M. (2022). Thermo-electro-mechanical characterization of pdms-based dielectric elastomer actuators. *Materials*, *15*(1). https://doi.org/10.3390/ma15010221

Kim, U. J. (2025). Preparation of Cellulose-Activated Carbon Gel with High Activated Carbon Content and Its Adsorption of Methylene Blue. *Nanomaterials*, *15*(11). https://doi.org/10.3390/nano15110799

Kundu, R., Mahada, P., Chhirang, B., & Das, B. (2022). Cellulose hydrogels: Green and sustainable soft biomaterials. In *Current Research in Green and Sustainable Chemistry* (Vol. 5). Elsevier B.V. https://doi.org/10.1016/j.crgsc.2021.100252

Li, M., Pal, A., Aghakhani, A., Pena-Francesch, A., & Sitti, M. (2022). Soft actuators for real-world applications. In *Nature Reviews Materials* (Vol. 7, Number 3, pp. 235–249). Nature Research. https://doi.org/10.1038/s41578-021-00389-7

Li, S., Gao, Z., Yang, W., Wang, R., & Zhang, L. (2025). Recent Advances in Dielectric Elastomer Actuator-Based Soft Robots: Classification, Applications, and Future Perspectives. In *Gels* (Vol. 11, Number 11). Multidisciplinary Digital Publishing Institute (MDPI). https://doi.org/10.3390/gels11110844

Li, S., Zhang, J., He, J., Liu, W., Wang, Y. H., Huang, Z., Pang, H., & Chen, Y. (2023). Functional PDMS Elastomers: Bulk Composites, Surface Engineering, and Precision Fabrication. In *Advanced Science* (Vol. 10, Number 34). John Wiley and Sons Inc. https://doi.org/10.1002/advs.202304506

Li, X., Li, L., Liu, X., & Hu, Y. (2025). Hydrogel actuators: from building blocks selection, anisotropic structures design to multifunctional applications. In *Soft Science* (Vol. 5, Number 3). OAE Publishing Inc. https://doi.org/10.20517/ss.2025.47

European Commission. (n.d.). *Life Cycle Assessment & the EF methods - Green Forum*. Life Cycle Assessment: The Scientific Foundation of the Environmental Footprint Methods. Retrieved April 26, 2026, from https://green-forum.ec.europa.eu/green-business/environmental-footprint-methods/life-cycle-assessment-ef-methods_en

López-Díaz, A., Vázquez, A. S., & Vázquez, E. (2024). Hydrogels in Soft Robotics: Past, Present, and Future. In *ACS Nano* (Vol. 18, Number 32, pp. 20817–20826). American Chemical Society. https://doi.org/10.1021/acsnano.3c12200

Methanol (M1770) - Product Information Sheet. (n.d.). Sigma.

Miao, W., & Bai, H. (2024). The new material science towards sustainable robotics. In *Journal of Materials Chemistry C* (Vol. 12, Number 33, pp. 12721–12733). Royal Society of Chemistry. https://doi.org/10.1039/d4tc01868k

Miranda, I., Souza, A., Sousa, P., Ribeiro, J., Castanheira, E. M. S., Lima, R., & Minas, G. (2022). Properties and applications of PDMS for biomedical engineering: A review. In *Journal of Functional Biomaterials* (Vol. 13, Number 1). MDPI. https://doi.org/10.3390/jfb13010002

Molla, M. H. O. R., Chen, J., & Xu, C. (2026). Advancing soft robotics: recent progress in dielectric elastomer and fluid actuators. *Npj Robotics*, *4*(1), 17. https://doi.org/10.1038/s44182-026-00074-3

Nasseri, R., Bouzari, N., Huang, J., Golzar, H., Jankhani, S., Tang, X. (Shirley), Mekonnen, T. H., Aghakhani, A., & Shahsavan, H. (2023). Programmable nanocomposites of cellulose nanocrystals and zwitterionic hydrogels for soft robotics. *Nature Communications*, *14*(1). https://doi.org/10.1038/s41467-023-41874-7

Park, C. S., Kang, Y. W., Na, H., & Sun, J. Y. (2024). Hydrogels for bioinspired soft robots. In *Progress in Polymer Science* (Vol. 150). Elsevier Ltd. https://doi.org/10.1016/j.progpolymsci.2024.101791

Protz, R., Lehmann, A., Ganster, J., & Fink, H. P. (2021). Solubility and spinnability of cellulose-lignin blends in aqueous NMMO. *Carbohydrate Polymers*, *251*. https://doi.org/10.1016/j.carbpol.2020.117027

Qian, L., Chen, C., Huang, Y., Ren, H., Cao, X., He, B., & Li, J. (2023). Nanocellulose-based electroactive actuators and their performance with various ions. *Cellulose*, *30*(7), 4455–4468. https://doi.org/10.1007/s10570-023-05143-6

Sala, S., Reale, F., & Cristobal-Garcia J. (2016). *Life cycle assessment for the impact assessment of policies Life thinking and assessment in the European policies and for evaluating policy options*. https://doi.org/10.2788/318544

Sales, F. C. P., Ariati, R. M., Noronha, V. T., & Ribeiro, J. E. (2021). Mechanical characterization of PDMS with different mixing ratios. *Procedia Structural Integrity*, *37*(C), 383–388. https://doi.org/10.1016/j.prostr.2022.01.099

selective coating, copper sheet, sputtering - Germany - selective coat, copper sheet, sputter deposition | ecoQuery. (n.d.). Retrieved May 3, 2026, from https://ecoquery.ecoinvent.org/3.11/cutoff/dataset/4893/documentation

Szabó, L., Milotskyi, R., Sharma, G., & Takahashi, K. (2023). Cellulose processing in ionic liquids from a materials science perspective: turning a versatile biopolymer into the cornerstone of our sustainable future. In *Green Chemistry* (Vol. 25, Number 14, pp. 5338–5389). Royal Society of Chemistry. https://doi.org/10.1039/d2gc04730f

Kraemer, R., Reyes, G., Cartes, M., Mejía, A., & Rojas, O. J. (2023). *Ionic liquid interactions with cellulose and the effect of water*. https://doi.org/10.21203/rs.3.rs-3213859/v1

Taokaew, S. (2023). Recent Advances in Cellulose-Based Hydrogels Prepared by Ionic Liquid-Based Processes. In *Gels* (Vol. 9, Number 7). Multidisciplinary Digital Publishing Institute (MDPI). https://doi.org/10.3390/gels9070546

Teixeira, I., Castro, I., Carvalho, V., Rodrigues, C., Souza, A., Lima, R., Teixeira, S., & Ribeiro, J. (2021). Polydimethylsiloxane mechanical properties: A systematic review. *AIMS Materials Science*, *8*(6), 952–973. https://doi.org/10.3934/matersci.2021058

Tube Revolver, Operation Manual 9240-11-021. (n.d.). Retrieved May 18, 2026, from https://www.thermofisher.com/order/catalog/product/88881001

Thermo Scientific Heratherm Heating and Drying Ovens Efficient, safe and easy thermoscientific. (n.d.).

Tjokro, K. (2023). *Life Cycle Assessment of microfluidic devices for point-of-care testing A comparative analysis of PDMS, paper and PLA*. http://repository.tudelft.nl.

Trombino, S., Sole, R., Di Gioia, M. L., Procopio, D., Curcio, F., & Cassano, R. (2023). Green Chemistry Principles for Nano- and Micro-Sized Hydrogel Synthesis. In *Molecules* (Vol. 28, Number 5). MDPI. https://doi.org/10.3390/molecules28052107

Wang, H., Du, J., & Mao, Y. (2025). Hydrogel-Based Continuum Soft Robots. In *Gels* (Vol. 11, Number 4). Multidisciplinary Digital Publishing Institute (MDPI). https://doi.org/10.3390/gels11040254

Wang, R., Cheng, C., Wang, H., & Wang, D. (2024). Swollen hydrogel nanotechnology: Advanced applications of the rudimentary swelling properties of hydrogels. In *ChemPhysMater* (Vol. 3, Number 4, pp. 357–375). KeAi Communications Co. https://doi.org/10.1016/j.chphma.2024.07.006

Zhang, Q., Yu, W., Zhao, J., Meng, C., & Guo, S. (2025). A Review of the Applications and Challenges of Dielectric Elastomer Actuators in Soft Robotics. In *Machines* (Vol. 13, Number 2). Multidisciplinary Digital Publishing Institute (MDPI). https://doi.org/10.3390/machines13020101

Zhang, Y., Adam, C., Rehnstrom, H., & Contera, S. (2024). Temporal evolution of mechanical properties in PDMS: A comparative study of elastic modulus and relaxation time for storage in air and aqueous environment. *Journal of the Mechanical Behavior of Biomedical Materials*, *160*. https://doi.org/10.1016/j.jmbbm.2024.106779

Zhang, Y., Liu, F., Zhang, J., Gao, W., Yu, J., & Wang, L. (2024). Supplementary information Life-cycle thinking based GREENNESS framework for advancing green chemistry: Case study with typical ionic liquids for cellulose dissolution and regeneration. *ACS Sustainable Chemistry & Engineering*.

Zhang, Y., Man, J., Liu, X., Li, S., Cao, B., Yu, L., & Tan, X. (2025). Soft robotic grippers: a review. In *Frontiers in Materials* (Vol. 12). Frontiers Media SA. https://doi.org/10.3389/fmats.2025.1692206

SUPPLEMENTARY INFORMATION

Table S1. Supporting inventory for 1 kg of 1-ethyl-3-methylimidazolium acetate

Flow	Amount	Unit	Flow type
1-ethyl-3-methylimidazolium acetate	1	kg	Product output
Dimethyl carbonate	0.53	kg	Material input
Acetic acid, 98% solution state	0.09	kg	Material input
1-ethylimidazole	0.57	kg	Material input
Electricity, high voltage	0.19	kWh	Energy input
Heat, district or industrial, natural gas	6.2	MJ	Heat input
Carbon dioxide, process	0.13	kg	Emission to air
Wastewater	0.05	kg	Waste treatment output

Caption: Table S1 presents the upstream inventory used to produce 1 kg of 1-ethyl-3-methylimidazolium acetate. This process was used as the ionic liquid proxy in the Cellulosic Hydrogel Actuator model. The inventory is based on the supplementary LCI data for lignocellulosic film production using 1-ethyl-3-methylimidazolium acetate (Freire Ordóñez, Rozaria, et al., 2025 (Supplementary material)). The related RSC Sustainability article describes the LCA of lignocellulosic films produced using this ionic liquid (Freire Ordóñez, Pontillo, et al., 2025).

Table S2. Scaled ionic liquid production inventory for 0.00755 kg ionic liquid per hydrogel actuator

Flow	Calculation	Scaled amount	Unit
Dimethyl carbonate	$0.53 * 0.00755$	0.004	kg
Acetic acid, 98% solution state	$0.09 * 0.00755$	0.00068	kg
1-ethylimidazole	$0.57 * 0.00755$	0.0043	kg
Electricity, high voltage	$0.19 * 0.00755$	0.00143	kWh
Heat, district or industrial, natural gas	$6.2 * 0.00755$	0.0468	MJ
Carbon dioxide, process	$0.13 * 0.00755$	0.000982	kg
Wastewater	$0.05 * 0.00755$	0.000378	kg

Caption: Table S2 shows the scaled upstream inventory associated with the ionic liquid input used in one 10 g Cellulosic Hydrogel Actuator. The scaling factor is the foreground ionic liquid input of 0.00755 kg per actuator. The original 1 kg inventory of ionic liquid is shown in Table S1.

Note: No ionic liquid recovery was modeled in the foreground system. Therefore, the ionic liquid was treated as consumed or lost during the laboratory-scale hydrogel preparation.

Table S3. Supporting inventory for 1 kg of 1-ethylimidazole production

Flow	Amount implemented in OpenLCA	Unit	Flow type
1-ethylimidazole	1	kg	Product output
Glyoxal	0.786	kg	Material input
Formaldehyde	0.408	kg	Material input
Ammonia	0.27	kg	Material input
Ethylamine	0.622	kg	Material input
Tap water	2.55	kg	Water input
Electricity	0.987	kWh	Energy input
Heat from steam	0.02	kWh	Heat input
Wastewater	2.55	kg	Waste treatment output
VOCs	0.408	kg	Emission output
Ethylene glycol monoethyl ether	0.786	kg	Output flow

Caption: Table S3 presents the supporting inventory for 1 kg of 1-ethylimidazole production. This process was used as an upstream precursor process for ionic liquid production. The material inventory is based on the supplementary LCI of imidazole derivative production reported by (Y. Zhang, Liu, et al., 2024).

Note: The table reports the values as implemented in the OpenLCA supporting process. The process was used as a foreground-supporting chemical inventory because an exact Ecoinvent dataset for this precursor route was not available.

Table S4. Foreground inventory for one 10 g Cellulosic Hydrogel Actuator

Process step	Input flows	Output flows	Calculation
Heating of ionic liquid	Ionic liquid: 0.00755 kg; Electricity: 0.00038 kWh; Transport: 12.08 kg*km	Heated IL: 0.00755 kg	Transport = 0.00755 * 1600
Mixing cellulose with IL	Heated IL: 0.00755 kg; Cellulose fibre: 0.00062 kg; Transport: 0.992 kg*km	Cellulose + IL: 0.00817 kg	Transport = 0.00062 * 1600
Hydrogel regeneration	Cellulose + IL: 0.00817 kg; Activated carbon: 0.00193 kg; Electricity: 0.001 kWh; Transport: 3.09 kg*km	Regenerated hydrogel: 0.01010 kg	Activated carbon treated as high-loading additive
Precipitation	Regenerated hydrogel: 0.0101 kg; Deionised water: 0.01 kg	Precipitated hydrogel: 0.01010 kg; Wastewater: 0.00001 m^3	Wastewater = 0.01 kg / 1000 kg * m^{-3}
Filtration	Precipitated hydrogel: 0.01010 kg	Filtered mix: 0.0101 kg	No additional foreground input
Washing	Filtered mix: 0.0101 kg; Deionised water: 0.01 kg	Washed mix: 0.0101 kg; Wastewater: 0.00001 m^3	Wastewater = 0.01 kg / 1000 kg * m^{-3}
Purification	Washed mix: 0.0101 kg; Deionised water: 0.01 kg	Purified mix: 0.0101 kg; Wastewater: 0.00001 m^3	Wastewater = 0.01 kg / 1000 kg * m^{-3}
Phase separation and gelification	Purified mix: 0.0101 kg; Deionised water: 0.01 kg	Gelled mix: 0.0101 kg; Wastewater: 0.00001 m^3	Wastewater = 0.01 kg / 1000 kg * m^{-3}

Shaping	Gelled mix: 0.0101 kg	Right shape material: 0.00712 kg; Inert waste: 0.00298 kg	Shaping loss = 0.0101 − 0.00712
Electrode coating and quality control	Right shape material: 0.00712 kg; Acrylic binder: 0.00268 kg; Deposited selective coating: 0.0002 kg; Transport: 4.928 kg*km	Stabilized material: 0.01 kg	Binder and coating added to shaped body
Final quality control	Stabilized material: 0.01 kg; Electricity: 0.0025 kWh	Cellulosic Hydrogel Actuator: 0.01 kg	Final output equals reference flow

Caption: Table S4 reports the foreground inventory for one 10 g Cellulosic Hydrogel Actuator. Values are primary foreground data from the OpenLCA model developed in this thesis. Supporting calculations are shown where values were derived from mass balance, water-density conversion, or transport assumptions.

Table S5. Geometrical and mass-based justification of binder and coating inputs

Parameter	Value	Unit	Calculation/explanation
One-sided actuator dimensions	120 * 24	mm	Assumed strip-like actuator geometry
One-sided surface area	28.8	cm^2	12 cm * 2.4 cm
Two-sided surface area	57.6	cm^2	2 * 28.8 cm^2
Two-sided surface area	0.00576	m^2	Area used for coating and binder calculations
Acrylic binder solution	2.68	g	OpenLCA foreground input
Dry acrylic binder solids	1.447	g	2.68 * 0.54
Water in acrylic binder solution	1.233	g	2.68 × 0.46
Wet binder layer thickness	0.465	mm	2.68 cm^3 / 57.6 cm^2
Dry binder layer thickness	0.251	mm	1.447 cm^3 / 57.6 cm^2
Selective coating area	0.00576	m^2	Ecoinvent area-based sputtering process input
Equivalent coating thickness	4	µm	Equivalent metallic layer thickness
Equivalent coating density	8700	kg/m^3	Metallic-density approximation
Deposited selective coating mass	0.0002	kg	A * t * ρ
Coating areal loading	3.47	mg/cm^2	0.20 g / 57.6 cm^2

Caption: Table S5 documents the geometrical and mass-based justification for the acrylic binder and selective coating inputs. The acrylic binder is interpreted as a structural adhesive/binder layer for electrode attachment and stabilization. The selective coating is interpreted as an equivalent deposited electrode/coating layer. The coating process itself was represented separately by an area-based Ecoinvent sputtering dataset (*Acrylic Binder Production, with Water, in 54% Solution State - Europe - Acrylic Binder, with Water, in 54% Solution State | EcoQuery*, n.d.).

Note: The acrylic binder dataset represents acrylic binder in a 54 wt% solution state, and the selective coating process is defined per square meter of coated area.

Table S6. Scaled inventory of acrylic binder production for 0.00268 kg binder solution

Flow	Amount per 1 kg acrylic binder solution	Scaled amount for 0.00268 kg	Unit	Flow type
Butyl acrylate	0.0901	0.000241	kg	Material input
Electricity, medium voltage	0.1	0.000268	kWh	Energy input
Esters of versatic acid	0.152	0.000407	kg	Material input
Heat, district or industrial	0.5225	0.0014	MJ	Heat input
Heat, district or industrial	0.566	0.00152	MJ	Heat input
Vinyl acetate	0.329	0.000882	kg	Material input
Water, unspecified natural origin	0.00046	0.00000123	m^3	Resource input
Waste paint	0.000062094	0.000000166	kg	Waste output
Waste paint	0.02994	0.0000802	kg	Waste output
BOD5, Biological Oxygen Demand	0.000018	$4.82 * 10^{-8}$	kg	Emission to water
COD, Chemical Oxygen Demand	0.00017	0.000000456	kg	Emission to water
Dissolved solids	0.00036	0.000000965	kg	Emission to water
DOC, Dissolved Organic Carbon	0.000011	$2.95 * 10^{-8}$	kg	Emission to water
Hydrocarbons, aliphatic	0.00007	0.000000188	kg	Emission to air

Suspended solids	0.000021	$5.63 * 10^{-8}$	kg	Emission to water
TOC, Total Organic Carbon	0.00004	0.000000107	kg	Emission to water

Caption: Table S6 shows the scaled background inventory for the acrylic binder input used in one actuator. The Ecoinvent dataset represents the production of 1 kg of acrylic binder with water in 54% solution state and was scaled to the foreground input of 0.00268 kg. The Ecoinvent documentation states that the product represents an acrylic binder in a 54 wt% water solution and is used in the production of acrylic paint. (*Acrylic Binder Production, with Water, in 54% Solution State - Europe - Acrylic Binder, with Water, in 54% Solution State | EcoQuery*, n.d.)

Note: This table reports the main input and output flows visible in the OpenLCA implementation. The full background supply chain is included through the linked Ecoinvent provider.

Table S7. Scaled inventory of selective coating process for 0.00576 m² coated area

Flow	Amount per 1 m²	Scaled amount for 0.00576 m²	Unit	Flow type
Argon, liquid	0.00328	0.0000189	kg	Material input
Chromium	0.0074	0.0000426	kg	Material input
Copper, cathode	0.081	0.000467	kg	Material input
Corrugated board box	0.0177	0.000102	kg	Packaging input
Diesel, burned in building machine	0.225	0.0013	MJ	Energy input
Electricity, medium voltage	3.47	0.01999	kWh	Energy input
Kraft paper	0.00056	0.00000323	kg	Packaging input
Light fuel oil	0.0062	0.0000357	kg	Energy/material input
Lubricating oil	0.00077	0.00000444	kg	Material input
Metal coating facility	$3.333 * 10^{-7}$	$1.92 * 10^{-9}$	item(s)	Infrastructure input
Nitrogen, liquid	0.00182	0.0000105	kg	Material input
Oxygen, liquid	0.00091	0.00000524	kg	Material input
Polyethylene, low density	0.00052	0.000003	kg	Packaging/material input
Tap water	7.236	0.04168	kg	Water input
Tin	0.00862	0.0000497	kg	Material input
Municipal solid waste	0.00341	0.0000196	kg	Waste output
Waste mineral oil	0.00077	0.00000444	kg	Waste output
Wastewater, unpolluted	0.00023	0.00000132	m³	Wastewater output
Water emission to air	0.00109	0.00000628	m³	Emission to air
Water emission to water	0.00615	0.0000354	m³	Emission to water
Selective coat, copper sheet, sputter deposition	1	0.00576	m²	Reference product

Caption: Table S7 shows the scaled inventory of the Ecoinvent selective coating process used for one actuator. The process is defined per 1 m² of coated copper sheet and was scaled to the

two-sided actuator coating area of 0.00576 m². The Ecoinvent dataset represents the coating of 1 m² copper sheet by sputtering with chromium and tin oxide. (*Selective Coating, Copper Sheet, Sputtering - Germany - Selective Coat, Copper Sheet, Sputter Deposition | EcoQuery*, n.d.)

Note: The Ecoinvent process was used as a proxy for sputtering-based electrode/coating deposition at the area level. The deposited coating mass of 0.00020 kg was modeled separately as a foreground assembly flow.

Table S8. Foreground inventory for one 10 g PDMS Actuator

Process step	Input flows	Output flows	Calculation
Auxiliary components production	Acrylic binder: 0.00268 kg; deposited selective coating: 0.0002 kg; transport: 4.608 kg*km	Auxiliary components: 0.00288 kg	Transport = 0.00288 * 1600
Deposited selective coating production	Selective coat, copper sheet, sputter deposition: 0.00576 m^2	Deposited selective coating: 0.0002 kg	Area-based sputtering proxy
PDMS mixing	Polydimethylsiloxane: 0.00966 kg; curing-agent proxy: 0.00097 kg; electricity: 0.001 kWh; transport: 17.008 kg*km	PDMS mixture, uncured: 0.01063 kg	PDMS ratio ≈ 10:1
Casting/shaping	PDMS mixture: 0.01063 kg; electricity: 0.005 kWh	Shaped PDMS, uncured: 0.01053 kg; waste plastic mixture: 0.0001 kg	Casting loss included
Thermal curing	Shaped PDMS: 0.01053 kg; electricity: 0.12 kWh	Cured PDMS blank: 0.01053 kg	Oven electricity for one actuator
Replica removal and trimming	Cured PDMS blank: 0.01053 kg	PDMS parts: 0.00712 kg; waste plastic mixture: 0.00341 kg	Trimming loss included
Surface cleaning	PDMS parts: 0.00712 kg; methanol: 0.0002 kg; deionized water: 0.001 kg; transport: 0.32 kg*km	Cleaned PDMS part: 0.00712 kg; wastewater: 0.000001 m^3; methanol emission to water: 0.0002 kg	Methanol transport = 0.0002 * 1600

Electrode application and final shaping	Cleaned PDMS part: 0.00712 kg; auxiliary components: 0.00288 kg	PDMS actuator, assembled: 0.01 kg	Assembly reaches final actuator mass
Cleaning	PDMS actuator, assembled: 0.01 kg; deionized water: 0.001 kg	PDMS actuator, cleaned: 0.01 kg; wastewater: 0.000001 m^3	Wastewater = 0.001 kg / 1000 kg/m^3
Stabilization	PDMS actuator, cleaned: 0.01 kg; electricity: 0.1 kWh	PDMS actuator, stabilized: 0.01 kg	Short oven stabilization step
Functional testing and finalization	PDMS actuator, stabilized: 0.01 kg; electricity: 0.0025 kWh	PDMS Actuator: 0.01 kg	Final output equals reference flow

Caption: Table S8 reports the foreground inventory for one 10 g PDMS Actuator. Values are primary foreground data from the OpenLCA model developed in this thesis. A generic organic chemical proxy was used as a surrogate for the curing agent because an exact curing-agent dataset was unavailable. The 10:1 PDMS base-to-curing-agent ratio is consistent with the technical data for SYLGARD 184 (Dow, 2017). A similar proxy approach for the PDMS curing agent was used in the Delft microfluidic device LCA, where “chemical, organic” was used as a proxy for the curing agent. (Tjokro, 2023)

Note: The electrical values for thermal curing and stabilization are assigned to a single actuator and are justified in the main LCI section using representative laboratory oven operation.

Table S9. Methanol input for PDMS surface cleaning

Parameter	Value	Unit	Explanation
Methanol input	0.0002	kg	Minimum practical solvent amount for cleaning one actuator
Methanol input	0.2	g	Converted from kg
Methanol volume	0.253	mL	Calculated using density of 0.7915 g/mL
Methanol emission to water	0.0002	kg	Full input assigned as emission flow

Table S9 presents the methanol input used for PDMS surface cleaning. The amount corresponds to approximately 0.25 mL per actuator and represents the minimum practical solvent quantity required for light wiping or degreasing before further processing (*Methanol (M1770) - Product Information Sheet*, n.d.).

Table S10. Transport inventory calculation for selected foreground flows

System	Transported flow	Mass	Calculation	Transport input
Hydrogel	Ionic liquid	0.00755 kg	0.00755 * 1600	12.08 kg*km
Hydrogel	Cellulose fibre	0.00062 kg	0.00062 * 1600	0.992 kg*km
Hydrogel	Activated carbon	0.00193 kg	0.00193 * 1600	3.09 kg*km
Hydrogel	Coating-related auxiliary materials	0.00308 kg	0.00308 * 1600	4.928 kg*km
PDMS	PDMS mixture materials	0.01063 kg	0.01063 * 1600	17.008 kg*km
PDMS	Auxiliary components	0.00288 kg	0.00288 * 1600	4.608 kg*km
PDMS	Methanol	0.0002 kg	0.0002 * 1600	0.32 kg*km

Caption: Table S10 presents the transport inputs used in the foreground inventory. Transport was calculated by multiplying the transported material mass by the assumed 1600 km delivery distance from Germany.

Note: The transport distance represents a consolidated delivery scenario from a central supplier region, not supplier-specific logistics for each material.

Table S11. Production-stage waste, wastewater, and emission flows

System	Flow	Amount	Unit	Origin	Explanation
Hydrogel	Wastewater	0.00004	m^3	Precipitation, washing, purification, gelification	Four water-processing steps, each using 0.01 kg water
Hydrogel	Inert waste	0.00298	kg	Shaping / trimming	Loss from forming the final hydrogel actuator shape
PDMS	Waste plastic mixture	0.00351	kg	Casting and trimming	Excess PDMS removed during molding and shape formation
PDMS	Wastewater	0.000002	m^3	Surface cleaning and final cleaning	Two cleaning steps, each using 0.001 kg water
PDMS	Methanol emission to water	0.0002	kg	Surface cleaning	Full methanol input assigned as emission flow

Caption: Table S11 summarises the production-stage waste, wastewater, and emission flows included in the foreground model. These flows represent fabrication losses and process outputs and do not describe the end-of-life treatment of the final actuators.

NON-EXCLUSIVE LICENCE TO REPRODUCE THE THESIS AND MAKE THE THESIS PUBLIC

I, Vjacheslav Morozov ,
(author´s name)

1. grant the University of Tartu a free permit (non-exclusive licence) to

   reproduce, for the purpose of preservation, including for adding to the digital archives of the University of Tartu until the expiry of the term of copyright, my thesis

   A Comparative Life Cycle Assessment of Hydrogel and Polydimethylsiloxane (PDMS) Actuators ,
   (title of thesis)

   supervised by Janno Torop, PhD; Alan Henry Tkaczyk, PhD; Cansu Özcan Kilcan, MSc ;
   (supervisor´s name)

2. grant the University of Tartu a permit to make the thesis specified in point 1 available to the public via the web environment of the University of Tartu, including via the digital archives, under the Creative Commons licence CC BY NC ND 4.0, which allows, by giving appropriate credit to the author, to reproduce, distribute the work and communicate it to the public, and prohibits the creation of derivative works and any commercial use of the work until the expiry of the term of copyright;

3. I am aware of the fact that the author retains the rights specified in points 1 and 2;

4. confirm that granting the non-exclusive licence does not infringe other persons' intellectual property rights or rights arising from the personal data protection legislation.

Vjacheslav Morozov

20/05/2026